

**INVESTIGATION OF OSTEOGENIC CHARACTERISTICS OF HUMAN  
ADIPOSE DERIVED STROMAL CELLS**

**MOHAN CHOTHIRAKOTTU ABRAHAM**

**(M. B, B. S)**

**A THESIS SUBMITTED FOR DEGREE OF MASTER OF SCIENCE (M Sc.)**

**DEPARTMENT OF SURGERY**

**FACULTY OF MEDICINE**

**NATIONAL UNIVERSITY OF SINGAPORE**

**2007**

## Table of Contents

**Preface**

**Acknowledgements**

**Summary**

**List of Tables**

**List of Figures**

|  |    |
|--|----|
| <b>Chapter 1 – Introduction</b>  | 1  |
| <b>Chapter 2 – Research Overview</b>                                     |    |
| 2.1 Aim and scope of thesis  | 3  |
| 2.2 Phase I of the study   | 5  |
| 2.3 Phase II of the study  | 6  |
| 2.4 Phase III of the study   | 6  |
| <b>Chapter 3 – Background and Literature Review</b>                      |    |
| 3.1 Basic concepts about stem cells                                      | 7  |
| 3.2 Mesenchymal stromal cells for tissue regeneration                    | 8  |
| 3.3 Adipose tissue as an alternative source of MSCs                      | 9  |
| 3.4 Characteristics of ADSCs   | 11 |
| 3.5 Biological and molecular mechanisms of osteogenic differentiation    | 13 |
| <b>Chapter 4 – Characterization of ADSCs in two-dimensional cultures</b> |    |
| 4.1 Introduction   | 20 |
| 4.2 Materials and Methods  | 21 |
| 4.3 Results  | 31 |
| 4.4 Discussion   | 43 |

|   |    |
|---|----|
| 4.5 Conclusion  | 47 |
| <b>Chapter 5 – RNA interference (RNAi) silencing of ATF5 in ADSCs</b>           |    |
| 5.1 Introduction  | 48 |
| 5.2 Materials and Methods   | 53 |
| 5.3 Results   | 56 |
| 5.4 Discussion  | 63 |
| 5.5 Conclusion  | 66 |
| <b>Chapter 6 – Co-Transfection and Expression of ATF4 and ATF5 in HEK cells</b> |    |
| 6.1 Introduction  | 67 |
| 6.2 Materials and Methods   | 70 |
| 6.3 Results   | 81 |
| 6.4 Discussion  | 86 |
| 6.5 Conclusion  | 88 |
| <b>Chapter 7 – Conclusion and Future line of work</b>                           | 90 |

## **PREFACE**

This work has been done as partial fulfillment of the Master of Science (MSc.) Degree, under the Faculty of Medicine, National University of Singapore. The work done in this thesis is original and no part has been copied or reproduced from elsewhere.

### ***Publication in peer reviewed journal***

Leong DT, **Abraham MC**, Rath RN, Lim TC, Chew FT, Hutmacher DW. Investigating the effects of preinduction on human adipose derived precursor cells in an athymic rat model

*Differentiation* 2006 Dec; 74(9-10) : 519-29

## ACKNOWLEDGEMENTS

*“A journey of a thousand miles begin with a single step”*

*- Chinese proverb*

No research work would be possible for a student to complete without the sincere and dedicated guidance of his or her mentors.

I am short of words when I have to express the profound gratitude that I have for my supervisor Dr Dietmar Werner Hutmacher. To me he epitomizes the perfect balance of a teacher and a friend. He has quite often forgiven me for my shortcomings and has given me the drive to go ahead in life. What I am now in life, I owe a lot to him – for his patience and understanding.

I would also like to express my sincere gratitude to Dr Jan Thorsten Schantz for having being a great supervisor and more than that, a good friend who would understand my ambitions and desires.

It would be heinous offence if I fail to acknowledge my “guru”, Dr Leong Tai Wei David, who was my senior in the lab. Whatever I have learnt and whatever I know in research, I have learnt from this great man. He has been a true friend, teacher and guide for the whole period of my graduate period. I consider myself extremely fortunate for having known him and having worked with such a towering, yet humble personality.

I would also like to express my gratitude to all my lab mates and friends, especially Dr Subh Narayan Rath and Dr Anurag Gupta for having helped me in times of crisis and confusions.

Last, but not least, I am grateful to all the people, both friends and family, who have stood with me in my toughest times and without whose prayers and efforts, I would have been able to make it to where I am.

Mohan C. Abraham

## SUMMARY

Adipose tissue is being considered as having a potential source for Mesenchymal stromal cells (MSCs) known as Adipose Derived Stromal Cells (ADSCs). In this work, ADSCs were isolated from lipoaspirates of human donors and their multipotentiality characterized by Histology, Immunohistochemistry, Real time PCR and Western Blot.

Previous work by Leong TWD had shown that that activating transcription factor 5 (ATF5) transcript level is down regulated during osteogenic differentiation of ADSCs. A close family member of ATF5, ATF4 is an important regulator of osteogenic differentiation in non-osteogenic cell lines. To further understand the role of ATF5 gene, ATF5 was silenced with RNAi and its effect on osteocalcin and ATF4 gene expression were measured with real time PCR. To study whether ATF4 and 5 are binding partners, HEK 293 cells were co-transfected with ATF4 and ATF5 plasmids and visualized with co-immunoprecipitation and immunoblotting.

It was seen that ATF5 silencing increased the expression of osteocalcin majority of donors' ADSC populations. However, ATF4 expression was not uniformly elevated in all the donor samples. Co-transfection and subsequent co-immunoprecipitation with immunoblotting of cell lysates with ATF4 and ATF5 antibodies demonstrated that immunoprecipitation of ATF4 results in simultaneous pull down of ATF5 and vice-versa. This it may be presumed that ATF4 might be able to interact with ATF5 in vivo. Therefore, ATF5 may have a role during the osteogenic differentiation of ADSCs by influencing the expression of osteogenic markers like osteocalcin through its interaction with ATF4.

## Table list

- Table 4.1** Primer sequence of genes used for real time PCR
- Table 5.1** Primer sequence of genes used for real time PCR in gene silencing experiment
- Table 6.1** Sequences used for generation of inserts

## Figure List

- Fig 3.1** Real time PCR for ATF5. Real time PCR done for ATF5 gene in twenty donor samples which were analyzed by gene chip expression analysis. A consistent drop in ATF5 is seen by the second day in all, but one, of the samples studied. (Adapted from PhD Thesis of Leong TWD)
- Fig 4.1** Morphology of ADSCs plated on tissue culture plastic. The initial morphology which is flat and polygonal (Fig 4.1A) changes to spindle shaped on continued culture (Fig 4.1B)
- Fig 4.2** Alizarin Red staining of ADSC. The uninduced samples (Fig 4.2A) do not take up any stain. Intense foci of mineralization seen in the induced samples (Fig 4.2B)
- Fig 4.3** Immunohistochemistry of osteogenic markers. Increased expression for the respective markers seen in the induced groups (B,D,E,F) compared to the uninduced group (A,C,E,G)
- Fig 4.4** Oil Red O stain for fat vacuoles. Fat vacuoles could be detected as early as day 14 in the induced samples (Fig 4.4A) and increased all the way up to day 28 (Fig 4.4B)
- Fig 4.5** FABP expression in ADSCs following adipogenic induction. The expression in day 14 samples (Fig 4.5A) and day 28 samples (Fig 4.5B) were similar in pattern, with increased expression seen in the induced samples
- Fig 4.6** LPL expression in ADSCs following adipogenic induction. The expression in day 14 samples (Fig 4.6A) and day 28 samples (Fig 4.6B) were similar in pattern, with a significantly increased expression seen in the induced samples
- Fig 4.7** Leptin expression in ADSCs following adipogenic induction at day 28. The expressions in day 14 samples were not detectable (data not shown).
- Fig 4.8** Osteocalcin expression. The levels of the gene were quite low in the day 14 samples (Fig 4.8A). However majority of the samples showed a significantly increased expression by day 28 (Fig 4.8B)
- Fig 4.9** Runx2 expression. The levels of the gene were quite low in the day 14 induced samples (Fig 4.9A). However, by day 28 a significantly increased expression was seen in the induced samples showed a significantly increased



expression by day 28 (Fig 4.9B)

- Fig 4.10** Osteopontin and osteonectin expression. In a few of the samples, the expression of osteopontin was much higher at 28 days of induction (Fig 4.10A) when compared to the day 14 samples. A similar profile was seen with osteonectin expression (Fig 4.10B)
- Fig 4.11** Western blots for osteogenic markers. Osteonectin and osteopontin expression (Fig 4.11 A and B) show a variable expression with time. This could be due to the fact that they are not very specific markers for osteogenesis. Fig 4.11 B1 and B2 show the two different isoforms of osteopontin obtained. As a control  $\beta$ -actin (Fig 4.11 C) and hFOBs cell line (Fig 4.11 D) were used
- Fig 5.1** ATF4 expression pattern in ADSCs. In three of the ten samples tested, the ATF4 expression increased during the second day and dropped drastically by the twenty-eight day. This pattern was similar to that seen with hFOBs cell lines. The lack of a consistent response in all the ADSC samples may be due to the differences in the ‘intrinsic osteogenic potential’ among the cells
- Fig 5.2** ATF5 expression normalized to  $\beta$ -actin. In all the donor samples tested there was a decreased expression of ATF5 in the gene silenced groups (*Ri +*). The time point at which silencing was maximum varied from sample to sample, with some having a pronounced response at day 1, while others having at day 2. (A representative graph of two donor samples are being shown in Fig 5.2 A and B).
- Fig 5.3** Osteocalcin expression normalized to  $\beta$ -actin. There were significant increases in the expression levels of osteocalcin in the gene silenced groups at varying time points (*Ri + subgroups*). All the samples showed increased expressions, at different time points, in the sub optimally induced (*O.IX Ri +*) and uninduced (*OX Ri +*) groups which were gene silenced. The arrow heads show the relevant time points at which significant differences were seen.
- Fig 5.4** ATF4 expression normalized to  $\beta$ -actin. Some of the ADSC samples showed an increased expression of ATF4 in the ATF5 silenced groups (arrow headed groups in Figs 5.4 A and B). However the significance was not observed across all the donor samples (data not shown).
- Fig 6.1** Vector map of pcDNA6/His<sup>TM</sup> A ([www.invitrogen.com](http://www.invitrogen.com))
- Fig 6.2** Multiple Cloning Site (MCS) of pcDNA6/His<sup>TM</sup> A ([www.invitrogen.com](http://www.invitrogen.com))

- Fig 6.3** Gel picture of the inserts obtained from PCR. ATF4 (Fig 6.3 A) corresponds to the 1050 bp marker, while ATF5 corresponds to 900 bp marker (Fig 6.3 B). Running the two inserts on the same gel gave a clearer distinction between the two (Fig 6.3 C). The one on the left is the ATF4 insert and the one on the right is the ATF5 insert.
- Fig 6.4** Gel picture of the vector after Restriction Enzyme digestion. The uncut vector (turquoise box) having a weight of 5200 bp, being supercoiled appears to run faster than the cut vector (red box). This is because the linear structure of the cut vector impedes its paces through the gel, causing it to appear lagging behind the uncut vector.
- Fig 6.5** Gel picture of the inserts obtained from colony PCR. ATF4 insert (Fig 6.5 A) within the plasmid corresponds to the 1100 bp marker, while ATF5 corresponds to 950 bp marker (Fig 6.5 B)
- Fig 6.6** Anti-His immunoblotting of the HEK lysates. The lysates obtained from cotransfected cells (Fig 6.6A) show three distinct bands at molecular weight 80, 70 and 65 kD. Cell lysates from single transfection with ATF5 (Fig 6.6B) show a single band at 65 kD. This can be compared to the lysates from untransfected control HEK cells (the areas shaded in the dark blue box) where no such bands could be seen.
- Fig 6.7** Anti-ATF5 and anti-ATF4 immunoblotting of the HEK lysates. The lysates obtained from cotransfected cells show a single prominent band at 65 kD when immunoblotted with anti-ATF5 antibody (Fig 6.7 A). Immunoblotting of the same blot with anti-ATF4 showed two prominent bands at about the same weight (Fig 6.7 B). This is in comparison to untransfected controls which do not show any such bands (the area shaded with the dark blue box)
- Fig 6.8** IP with anti-ATF4; WB with anti-ATF5. The immunoblotting with anti-ATF5 showed the presence of two prominent bands. The heavier band was at molecular weight of 65 kD, while the lighter one was at around 32 kD.
- Fig 6.9** IP with anti-ATF5; WB with anti-ATF4. The immunoblotting with anti-ATF4 showed the presence of a single, distinct band of molecular weight 35 kD.

## **CHAPTER 1**

### **INTRODUCTION**

A variety of clinical conditions require bone regeneration. It has been estimated that currently around 20 % of fractures fail to heal properly (Verettas DA et al., 2002) which include scenarios like non-union, malunion and trauma. Currently the problem that is being faced is finding an ideal source for repairing bone tissue. The most widely used method for bone reconstruction is autologous graft, but the volume of tissue that can be obtained is limited by complications like morbidity, bleeding, infection and chronic pain (Kimelman G et al., 2007).

Interest is currently being focused on the use of stem cells and precursor cells for this purpose. The two types of stem cells that are being targeted for use in tissue regeneration are the Embryonic stem cells and the Adult stem cells. The embryonic stem cells, being restricted by ethical issues regarding their use, are being sidelined and focus is shifting to their adult counterparts (Yoon E et al., 2007).

One potential reservoir for a good source of multipotent adult stem cells is the adipose tissue. Cells isolated from these, known as ADSCs (Adipose Derived Stromal Cells) have been shown to possess the property of being multipotent and can give rise to cells types of different lineages, including those of the osteogenic lineage (Zuk PA et al., 2002).

Compared to the other sources of adult stem cells, these cells are found in large numbers and can be easily isolated and propagated in culture.

ADSCs have been quite well characterized by several groups in both two and three dimensional environments (Leong DT et al., 2006; Majumdar MK et al., 2003). In vivo experiments with osseous defects have shown their ability to regenerate bone tissue, which integrate well with the surrounding bony areas and retain the properties of native bone (Cowan CM et al., 2004). ADSCs transfected with recombinant bone morphogenic proteins (BMP-2) have shown to have better viability and a greater ability for depositing calcific matrices (Dragoo JL et al., 2003).

With widespread application being projected for ADSCs in orthopedic and craniofacial bone repairs, a better and clearer understanding of the mechanisms that dictate the osteogenic differentiation of ADSCs is required as such an understanding would thus serve to develop applications with more specific targets.

## CHAPTER 2

### RESEARCH OVERVIEW

#### 2.1 Aim and scope of the thesis

Differentiation and lineage commitment of precursor cells are regulated by the expression and repression of a number of genes. Preliminary transcriptome analysis of ADSCs collected from twenty patients in our group (PhD Thesis of Leong TWD) had shown that following the process of osteogenic induction, several genes in these cells undergo varying folds of expression. Among them, one gene known as ATF5, otherwise known as Activating Transcription Factor 5, was found to be consistently down regulated in all the twenty donor samples analyzed. This was further validated by real-time PCR analysis of mRNA samples from these twenty donors (Fig 3.1). As can be seen in the figure, the ATF5 levels drop drastically by the second day of induction in all, but one, of the twenty samples.

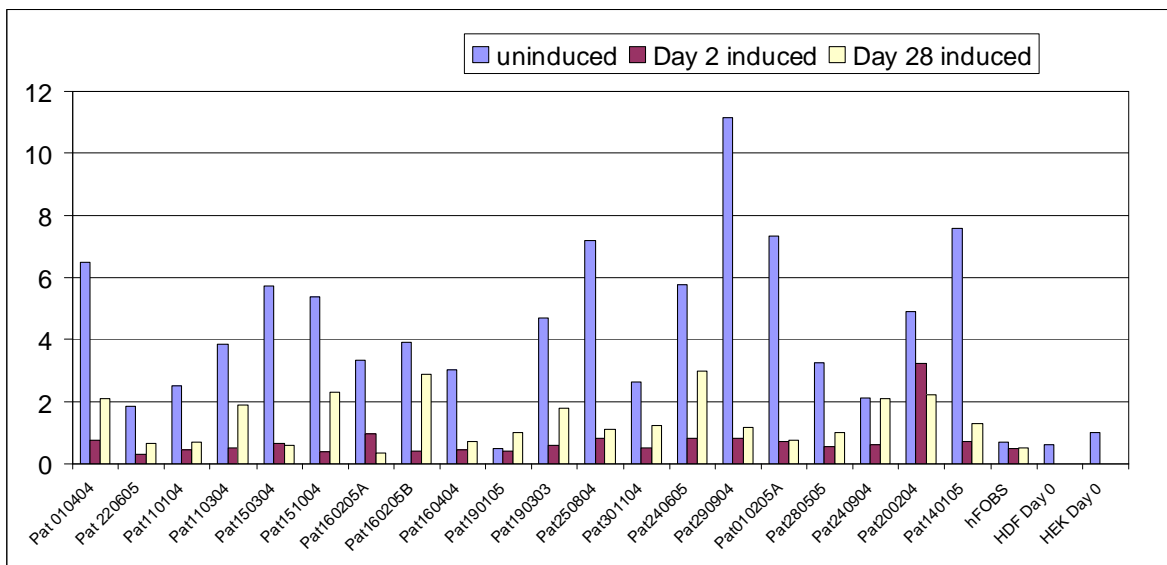


**Fig 2.1 – Real time PCR for ATF5.** Real time PCR done for ATF5 gene in twenty donor samples which were analyzed by gene chip expression analysis. A consistent drop in ATF5 is seen by the second day in all, but one, of the samples studied. (Adapted from PhD Thesis of Leong TWD)

ATF5 belongs to the family of cAMP binding elements having a leucine zipper motif (Hai T et al., 2001). ATF5 has been shown to have a major role in oligodendrocyte differentiation and astrocytic maturation of neural precursor cells (Angelastro et al., 2005) and is seen in very high levels in glioblastoma cell lines. However, no definite role of ATF5 in bone formation has been shown to date.

As mentioned earlier, ATF4 levels are elevated in osteoblasts and they induce osteogenic expression in non-osteoblast cells (Yang X et al., 2004b), which might imply that this transcription factor could have a significant role in non-osteoblast precursor cells like ADSCs when they are exposed to osteogenic stimuli. This fact, coupled with our observation of a consistent down regulation of its family member, ATF5, during osteogenic differentiation of ADSCs prompted us to consider that these two proteins maybe interacting with each other in the uninduced, native state of the ADSCs. When ADSCs are exposed to an osteogenic stimulus, this interaction might be altered, leading to the gene expression pattern that was observed. Members of the ATF family have been known to interact with each other and with a host of other transcription factors in forming homodimers and heterodimers (Ameri K et al., 2007). It might be possible that ATF5 down regulation during osteogenic induction in ADSCs could be directly or indirectly coupled to ATF4 expression and accumulation in these cells. On the contrary, it might equally be possible that ATF5 down regulation during osteogenic induction may be a phenomenon that is totally independent and unlinked to ATF4 expression.

However, we decided to explore the possibility that the reciprocal expression of the two proteins might be linked to each other. The hypothesis in this matter was that ATF5 might be interacting with ATF4 in uninduced native ADSCs, keeping the function of the latter protein repressed, and that following osteogenic induction, the ATF5 down regulation that we have observed might serve to derepress the functions of ATF4.

As a preliminary step towards understanding these phenomena, we first looked for the expression of ATF4 in the same group of ADSCs which showed a consistent down regulation of ATF5. Subsequently, ATF5 expression was silenced in ADSCs using RNA Interference strategies, and the consequent expression pattern of osteocalcin, a unique marker for osteogenic maturation, and ATF4 were seen. In order to find if ATF4 and ATF5 have the ability to interact with each other, these two genes were cloned into mammalian expression vector (pCDNA6/His<sup>TM</sup> A vector) and transfected into HEK 293 cells for protein expression. Co-immunoprecipitation was subsequently done on the cells lysates to see if the two proteins were capable of interacting with each other.

## **2.2 Phase I of the study**

As a preliminary run up to the major study, ADSCs were isolated from the lipoaspirates of patients coming to the hospital for cosmetic surgery. These cells were then assessed for their differentiation potential by putting them through a round of induction with osteogenic and adipogenic induction cocktails. The extents of differentiation were analyzed by histology, immunohistochemistry, real-time PCR and Western blots.

### **2.3 Phase II of the study**

In this phase, a total of ten samples, representative of the group of ADSCs studied by Leong TW David, were put through a 28 day induction period and the total RNA isolated to analyze the expression pattern of ATF4 gene under osteogenic influences. Subsequently ATF5 gene expression were silenced in four ADSC samples, by using RNA interference (RNAi) techniques and the expression pattern of ATF4 and one of the most specific markers of osteogenesis, osteocalcin were analyzed. This phase would thus give an indication as to how the expression patterns of ATF4 and osteocalcin would be varying under the conditions of ATF5 repression and osteogenic induction.

### **2.4 Phase III of the study**

In the final phase of the study, ATF4 and ATF5 genes were cloned in mammalian expression vector and transfected into HEK (Human Embryonic Kidney) 293 cell lines. Once these cells expressed the two proteins, they were isolated and immunoprecipitation was done on the expressed lysates to look for any interaction between the two proteins.



## **CHAPTER 3**

### **BACKGROUND AND LITERATURE REVIEW**

The advent of stem cells upon the horizon of modern medicine has opened up a new arena for advancing the therapeutic potential of regenerative medicine. The unique property of these cells have made them the subject of extensive research, with the hope that one day they could be used as a significant source for any type of tissue replacement. Though much hope is being placed upon stem cells as the ultimate cure for several debilitating illnesses, a profound understanding of the fundamental mechanisms that govern their growth and differentiation is needed before their full therapeutic repertoire could be exploited.

#### **3. 1. Basic concepts about stem cells**

Stem cells are a population of cells within the body having the unique capability of multiplication while at the same time maintaining self renewal and being able to give rise to tissues of different lineages when exposed to the right conditions (Grove J et al., 2004; Pomerantz J et al., 2004). This ability of stem cells to give rise to a variety of native cell types makes them promising candidates for the treatment to chronic ailments like Parkinson's disease, diabetes, stroke and cardiac damage. Presently there are two well defined types of stem cells – the embryonic stem cells and the adult stem cells. The embryonic stem cells, which are found within inner cell mass of the embryonic blastocyst, is by far considered the most appropriate type which fits into the definition of

the stem cells. Embryonic stem cells have been shown to be totipotent i.e. having the ability to differentiate into virtually any cell within the human body. They can be grown in relatively large quantities in culture, which would make it an ideal cell source for cell replacement therapies. The versatility of the embryonic stem cells are mired by the fact that their multipotency makes them rather unstable, forming tumorous masses when grown in vivo. This combined with the ethical issues of procuring these cells from live embryos have curbed its popularity as a possible source of stem cells for therapeutic purposes. Attention is now being focused on a distinct population of cells which are found at various sites in the adult body, known as the adult stem cells. The adult stem cell type which has been well characterized and studied is the hematopoietic stem cell (HSC). Studies have shown that the HSCs are also multipotent and quite capable of being plastic. Another type of adult stem cell which has been in the limelight for quite a while and is being extensively studied for cell replacement therapies is the Mesenchymal stem cell variably called Mesenchymal stromal cells (MSCs).

### **3.2. Mesenchymal stromal cells for tissue regeneration**

MSCs are cells of mesodermal origin and have been shown to be undifferentiated while at the same time having the ability of self renewal, remarkable proliferation potential and ability to differentiate into cell types of mesodermal and non-mesodermal origin (Pittenger MF et al., 1999). Although the bone marrow has been traditionally considered as the major source for MSCs, they can also be isolated from other sites like the cartilage, epithelium etc, albeit, at much lower numbers. The multilineage differentiation potential of these cells have been well established and they have been demonstrated to differentiate

into cells of both mesodermal and non- mesodermal origin like hepatic , neuronal and skeletal muscle types (Ong SY et al., 2006, Krabbe C et al., 2005, Gornostaeva SN et al., 2006). Banking on the bone marrow as the sole source of MSCs for therapeutic purposes has its own limits. The major drawback is that proportion of MSCs in the bone marrow is very low – estimated at around one cell in 18,000 nucleated cells per ml of bone marrow (Muschler GF et al., 2001). This number could not be augmented by aspirating more bone marrow; as such a procedure would impede some of the other important functions, like hematopoiesis and granulopoiesis, which take place in the bone marrow (Muschler GF et al., 2001). The morbidity and complications associated with tapping the bone marrow for these cell aspirates have also contributed to the search of alternative sources for adult stem cells.

### **3.3. Adipose tissue as an alternative source of MSCs**

Another important source of MSCs which could be tapped significantly without much morbidity to the patient and holds promise in tissue repair and regeneration is the adipose tissue. Adipose tissue is a mesoderm derivative and contains a varied stromal population, encompassing microvascular endothelial cells and even smooth muscle cells and a type of precursor cells called Adipose tissue derived cells (ADSCs) (Zuk PA et al., 2001). These cells have variably been known as Processed Lipoaspirate (PLA), adipose tissue derived progenitor cells, adipose derived stem cells etc, all denoting a lack of consensus among the taxonomists. These cells are isolated from the adipose tissue removed during the process of liposuction done for cosmetic purposes and proliferated in large numbers under standard conditions of culture (Zuk PA et al., 2001). A significant edge these cells

possess over their bone marrow counterparts is their relatively larger proportion in the adipose depot. ADSCs are known to exist in a proportion of around 2 % of the nucleated cell population in adipose tissue (Strem BM et al., 2005). With the earlier mentioned frequency of precursor cells in bone marrow, a typical bone marrow aspirate would not yield more than  $2 \times 10^4$  MSCs in a mature adult (Muschler GF et al., 2001). This contrasts to the estimated frequency of roughly  $1 \times 10^6$  MSCs obtained from a typical harvest of around 200 ml of adipose tissue, obtained during a normal liposuction under local anesthesia (Aust L et al., 2004). Thus, the adipose tissue has a phenomenal advantage over the bone marrow in terms of the magnitude of available MSCs. Apart from this feature, the ADSCs have been shown to possess multilineage differentiation potential, with capability of differentiation into multiple lineages (Ashjian PH et al., 2003; Mizuno et al., 2002). Several groups have shown that when ADSCs are exposed to a fixed combination of 1, 25 Dihydroxycholecalciferol,  $\beta$  – glycerophosphate and ascorbate (Zuk PA et al., 2002), they begin to express markers of osteogenesis, like collagen I, osteocalcin, CBFA -1 and alkaline phosphatase. Under the influence of a different induction medium, they begin to express markers of cartilage formation like collagen II, aggrecan and SOX 9 (Bernardo ME et al., 2007).

Not only have ADSCs been shown to differentiate into other mesenchymal tissues like liver (Talens-Visconti R et al., 2007) and pancreas (Timper K et al., 2006) , but also have the capability to cross the lineage barrier and form ectodermal tissues like neurons (Ashjian PH et al., 2003)

### 3.4. Characteristics of ADSCs

The ADSCs are very much similar to their counterparts in the bone marrow in terms of phenotypic qualities and expression of certain cell surface markers (Minguell JJ et al., 2001; Gronthos S et al., 2001). ADSCs also have the property of plastic adherence, which forms the basis of the usual method of isolating them. Even then, the populations of ADSCs are fairly heterogeneous (Barry FP et al., 2004) and this property alone cannot be used for the screening and purification of MSCs. One of the methods to enrich a native cell population is to look for surface markers, which when screened in certain fixed combinations, could be used as a unique signature for distinct cell populations. The ADSCs are uniformly positive for some of the hallmark MSC receptors like STRO-1 and CD 166 (Majumdar et al., 2003). The STRO-1 is a marker for undifferentiated MSCs and is lost once the cells are committed towards the osteogenic pathway (Bruder SP et al., 1997), while CD 166 has been postulated to play a significant role in osteogenic differentiation (Bruder SP et al., 1998). The ADSCs uniformly expressed HLA-ABC, CD 90 (Thy-1), CD 29 (integrin  $\beta 1$ ) which is an important marker for angiogenic potential; CD 49b and CD 49 d, both of which belong to the integrin- $\alpha$  group of molecules. These molecules have been best studied in the bone marrow MSCs and when occurring in a certain combination over the cell surfaces, they could interact with components of the extracellular matrix like fibronectin ( $\alpha 3\beta 1$ ), collagen ( $\alpha 1\beta 1$  and  $\alpha 2\beta 1$ ), laminin ( $\alpha 6\beta 1$  and  $\alpha 6\beta 4$ ) and vitronectin (Verfaillie et al., 1994). In ADSCs too they are essential for the development of the extracellular matrix and cell adhesion (Li TS et al., 2005; Katz AJ et al., 2005; Strem BM et al., 2005). The function of these receptor molecules in MSCs are not just restricted to adhesion; through their interaction with

extracellular matrix proteins like laminins, collagen, vitronectin, they play a key role in regulate cell proliferation and directing differentiation (Klees RF et al., 2005; Salaszyk RM et al., 2004).

Other molecules expressed by ADSCs include, CD 55; CD 59 and CD 105. On the other hand they do not express any of the markers of the hematopoietic lineage like CD 45 or CD 31 (De Ugarte DA et al., 2003) or other markers of angiogenesis like CD 106 (VCAM-1), CD 117 (c-kit), CD 133 and ABCG2 and HLA-DR. While this may be true of the ADSCs which have been in culture for a while, some groups have shown that ADSCs which are freshly harvested from the adipose tissue have an apparently different profile. These cells possess the hematopoietic markers like CD 34, CD 133 and ABCG2, which decrease after culturing for 3 to 5 days. Others have shown that CD 34 is a marker predominantly seen in the mature fraction of the adipocyte population (Festy F et al., 2005).

ADSCs are similar to the bone marrow MSCs in mediating immunomodulatory effects. They have been shown to secrete soluble factors that suppress the proliferation and inflammatory cytokine production in T cells and even control the GVHD (Graft versus Host Disease) in allogenic bone marrow transplantation in animal models (Yanez R et al., 2006). They constitutively produce certain cytokines like IL 6, 11, SCF (stem cell factor), LIF (leukemia inhibitory factor) M-CSF and G-CSF when grown in normal media, but the expression profiles of these cytokines change when grown in the presence of substances like dexamethasone (a potent osteogenic inducer) and IL 1 , indicating that the

cytokines produced by these stem cells could determine the extent of differentiation and growth potential of them (Haynesworth SE et al., 1996).

### **3.5. Biological and molecular mechanisms of osteogenic differentiation**

Bone formation has been thought to occur by lineage specific differentiation of a pool of precursor cells, which under the influence of environmental and molecular signals commit themselves to this particular lineage (Caplan AI., 1994). These multipotent precursor cells were first shown to exist in bone marrow (Pittenger MF et al., 1999), but cells with similar properties were identified in the adipose tissue (Zuk PA et al., 2001) and have become well established source of cells for bone tissue engineering. Although ADSCs are being used extensively for bone regeneration, the molecular mechanisms that govern their differentiation towards the osteogenic lineage have not been completely elucidated and are just beginning to be unraveled. The earliest evidence indicating the probable existence of bone forming cells in adipose tissue came from observing patients with the disorder – progressive osseous heteroplasia – a condition in which calcific nodules were seen in the subcutaneous tissue (Shore EM et al., 2002) Since then, several groups have shown the ability of adipose tissue derived precursor cells to express markers of osteogenesis. In the native adipose tissue it has been shown that adipogenic differentiation is initiated by two transcription factors, C/EBP $\beta$  and C/EBP $\delta$ . These factors activate the expression of PPAR $\gamma$ , which finally drives the preadipocytes into mature adipocytes (Wu Z et al., 1996; Tontonoz P et al., 1994).

Molecular events that converge towards directing the differentiation of ADSCs to the osteogenic lineage also decrease their concomitant capacity for adipogenic differentiation. Signaling pathways mediated by BMP-2 is such a regulator of osteogenesis and exposure to BMP-2 signals represses adipocyte differentiation and promotes expression of osteoblast markers in preadipocytes (Skillington J et al., 2002). These patterns follow the established norm that the fundamental criteria for a cell's commitment to a particular lineage of maturation is the activation of one set of transcription factors and the repression of another set (Black BL et al., 1998; Karsenty G et al., 2002).

A proper understanding of some of transcription factors involved in osteogenesis could serve as a template for charting out the pathways for similar events in ADSCs. Bone formation involves the differentiation of precursor cells towards the formation of osteoblasts. The osteoblast is primarily considered at the body's bone-forming cell and differentiation along the osteogenic lineage involves the sequential expression of osteoblast-specific markers like osteocalcin (Ducy P et al., 1997), bone sialoprotein (BSP) and a variety of non-specific bone matrix proteins like osteopontin, alkaline phosphatase etc. (Owen TA et al., 1990). The key transcriptional regulator in osteoblast differentiation is the factor called Runx2 which is otherwise known as Cbfa1 (Ducy P et al., 1997). Cbfa1/Runx2 are homologs of the Runt family of transcription factors found in the *Drosophila* (Gergen JP et al., 1985) and is widely considered as the master transcription factor mediating osteogenesis (Ducy P et al., 1997) in progenitor stem cells. Runx2 knockout mice have been shown to display a complete absence of mineralized



bone, while the cartilage formation is not affected (Komori T et al., 1997). The target genes for Runx2 are those expressed by the mature osteoblasts namely, osteocalcin, osteopontin, BSP and collagen alpha I. Forced expression of Cbfa1 in non-osteoblast cells also resulted in the expression of the above markers, all demonstrating the central role of this transcription factor (Ducy P., 2000).

One of the most important pathways that has been proven to have a profound effect in modulating osteogenesis the one mediated by BMP-2 (Bone Morphogenic Protein-2). BMP belongs to the TGF  $\beta$  super family and were initially discovered by the ability of bone extracts to ossify tissues in non-osseous sites (Hogan BL., 1996 b). BMPs not only influence postnatal bone remodeling, but they have been shown to play a significant role in skeletal patterning during the embryonic stage (Hogan BL., 1996 a). BMPs induce the formation of both bone and cartilage, thereby placing their possible point of modulation on a common skeletogenic precursor cell (J Sodek et al.). BMPs mediate their effects broadly through two specific transmembrane receptors, BMP receptor types I and II. Following the binding of the ligands to the receptors, they undergo dimerization, resulting in activation of the receptor's intrinsic serine/threonine kinase mechanism, which phosphorylates the receptor specific Smads (Chen D et al., 2004). Intracellular Smad 1 and Smad 5 then migrate to the nucleus and regulate the transcription of genes involved in promoting osteogenesis like Cbfa1/Runx2 (Hanai J et al., 1999) and Dlx5 (Lee MH et al., 2003) which act directly on downstream target genes like osteocalcin, osteonectin and collagen either by itself or, as more recently shown, through a downstream regulator like osterix.

The exact mechanisms by which osterix regulates osteogenesis is unknown, but it functions downstream to Runx2 (Kobayashi T et al., 2005). This transcription factor belongs to the Sp gene family, which like other members of this family, contains three zinc finger DNA binding domains (Philipsen S et al., 1999). The importance of osterix was also shown by the total lack of bones in osterix null mice. Osterix has been thought of as a factor which acts at the juncture of osteo-chondro pathways and directs precursor cells away from chondrogenic and towards the osteogenic lineage (Nakashima K et al., 2002). Both Runx2 and osterix levels are elevated by BMP-2 treatment, pointing out to a region of convergence here (Kobayashi T et al., 2005). BMP-2 alone is not the only mediator which affects Runx2 expression. Other factors like FGF (Fibroblastic Growth Factor) and TGF-B 1 have been proposed as transcriptional mediators of Runx2 in the early stages of cellular commitment to differentiation (Choi KY et al., 2005)

Yet another important regulator of osteogenesis is the action of Vitamin D<sub>3</sub>. Though Vitamin D<sub>3</sub> has an effect on increasing the intestinal absorption of both calcium and phosphorous, it also has a direct effect on regulating osteogenic transcription, through the action of its receptor VDR (Christakos S et al., 2003). This receptor has functional DNA binding domain, through which it mediates its action within the cellular nucleus and a Ligand binding domain, which binds to other transcription factors like RXR, DRIP, and CBP etc. Among them, RXR plays a significant role in promoting VDR accumulation within the nucleus and prevents its export from the same (Prufer K et al., 2002). The complex of VDR-RXR and other co-factors bind to VDRE (Vitamin D Response Elements) on the DNA and trigger transcription of important osteogenic genes like

osteocalcin (Price PA et al., 1980) and Cbfa1/Runx2 (Drissi H et al., 2002). Other transcription factors which have been demonstrated to have an effect on osteoblast differentiation include Msx1, Msx 2, Twist, estrogen and androgens (Kobayashi et al., 2005).

One particular gene, known as ATF4, has the ability to induce osteogenic gene expression among non-osteoblast cells (Yang X et al., 2004a and b), which puts it along with Runx2 and osterix as the only other two genes which have so far been shown to possess this property (Karsenty G et al., 2002) . ATF4 has been known to regulate the terminal differentiation of osteoblasts and its deficiency has been implicated in the pathogenesis of Coffin-Lowry syndrome, a condition in which there is mental retardation associated with skeletal abnormalities (Yang X et al., 2004a). In osteoblasts, ATF4 is a substrate required for the phosphorylation of RSK2 enzyme and deficiency of this phosphorylated form of RSK2 has been implicated in Coffin-Lowry syndrome. ATF4, also known as cREP2 (c-AMP response element protein 2), RAXREB67 or C/ATF belongs to the family of cAMP binding elements having a basic leucine zipper motifs (bZIP). They interact with DNA through these domains and have been known to dimerize forming homodimers, heterodimers or even both (Hai T et al., 1991). A few other members of this large family include ATF1, ATF3, ATF6 and ATF5 (also known as ATFX), all of which have similar functions in mediating cellular homeostasis (Hai T et al., 2001).

ATF4 was initially thought of as being a transcriptional repressor (Karpinski et al., 1992), however it also has significant transcriptional activation functions in a variety of tissues. Some of the genes that are induced by this transcription factor includes, RANKL and Runx2 (Ameri K et al., 2007). Though ATF4 is not a specific transcription factor restricted to the osteoblasts, its relevance in bone formation cannot be undermined, as targeted disruption of this gene in mice causes osteoporosis and lethal dwarfism (Yang X et al., 2004). Like Runx2, ATF4 also binds to promoter region of osteocalcin. While Runx2 binds to the OSE 2 element of the promoter, ATF4 binds to a specific cis-acting element known as OSE1 to trigger osteocalcin expression (Xiao G et al., 2005). The exact roles played by each of these proteins in osteocalcin regulation have not been clearly outlined, but it has been shown that ATF4 interacts co-operatively with Runx2 in mediating osteocalcin expression.

ATF4 has a ubiquitous genetic expression, being expressed in a variety of tissues like brain, kidney, heart, testis etc. and has a significant roles in hematopoiesis (Masuoka HC et al., 2002) and differentiation in male external genitalia (Fischer C et al., 2004). Though the genetic expression of this transcription factor is widespread, the active protein form of ATF4 is found only in the mature osteoblasts (Yang X et al., 2004). The specific accumulation of ATF4 in osteoblasts has been thought to be due to the absence or decreased expression of  $\beta$ -TrCP, an ubiquitin mediated proteasomal pathway, in osteoblasts. This pathway functions to prevent the accumulation of this protein in non-osteoblast cells. In fact silencing of this pathway by RNA interference methods has shown the accumulation of ATF4 and osteocalcin in non-osteoblast cells (Yang X et al., 2004).

Runx2 has been known to form complexes with several signaling molecules in generating osteoblast specific responses. It has been found to interact with other proteins like Rb protein and TAZ in inducing osteoblast differentiation (Thomas DM et al., 2004). Likewise, Runx2 forms complexes with SMADs in mediating BMP induced osteoblast differentiation (Zhang YW et al., 2000). Such an interaction has also been found in the case of ATF4 and Runx2. Presence of ATF4 has been shown to enhance Runx2 activity and cotransfection studies with these two proteins have shown that they can form complexes in vivo (Xiao G et al., 2005).

Thus a variety of transcription factors like Runx2, ATF4 and osteocalcin interact with each other through a myriad of mechanisms and complexes to induce the pathways leading to osteogenesis.

## **CHAPTER 4**

### **CHARACTERIZATION OF ADSCs IN TWO-DIMENSIONAL CULTURES**

#### **4.1 INTRODUCTION**

Several groups have shown that the adipose tissue is an excellent source of progenitor cells. Not only are these cells abundant in the adipose tissue, but they too like the bone marrow MSCs, possess the property of multipotentiality. They have been shown to be capable of being induced along the osteogenic (Zuk et al., 2002), chondrogenic (Zuk PA et al., 2002) and even the myogenic lineages (Di Rocco G et al., 2006). The ease of availability of adipose tissue as a store house of these cells gives them a unique advantage over the bone marrow as a source of cells for the purpose of tissue regeneration. The fundamental problem that has been put forward, when using adipose tissue as a source for MSCs, is the extent of homogeneity of the progenitor cell population. Since they are primarily obtained by aspiration of subcutaneous adipose tissue, they could be potentially mixed with a lot of other native cell types like endothelial cells, smooth muscle cells etc. This problem has partly been alleviated by the property of ADSCs to adhere to a plastic surface. Culture techniques, whereby one plates these entire lipoaspirate of cells into a culture flask and selectively culture only the adherent population of cells, have shown that this adherent population is indeed the progenitor cell population of adipose tissue.

In this section the differentiation potential of these ADSCs in the two-dimensional environment of tissue culture plastic were studied, so as to establish that the cells obtained from the adipose tissue of liposuction samples were truly the progenitor cell population. For this purpose the cells were grown up to confluence and were induced along both the osteogenic and adipogenic pathway using a set of induction cocktails. In the process, their differentiation potential was assayed using histology, real time PCR techniques and western blot analysis for lineage specific proteins.

## **4.2 MATERIALS AND METHODS**

### **4.2.1 Tissue preparation and culture**

Lipoaspirates were obtained from abdominal regions of healthy adult donors after informed consent and approval by the Institutional Review Board, National University Hospital, through vacuum pump-assisted liposuction. Following this, the tissues samples were processed as per the protocol of Zuk et al. Briefly the tissue samples were first broken down manually in a coarse sieve and washed several times in sterile phosphate buffered saline (PBS). The washed tissue specimens were then dissociated with 0.075 % collagenase type I for 2 hours at 37° C. Following this about 10 ml of DMEM was added to the treated tissues, so as to inhibit the action of collagenase. The digested specimen was then centrifuged at 1200 x g for 10 minutes to form a cell pellet. The overlying layer of fat and debris were removed and the cell pellet was plated onto tissue culture plastic. Cultures were washed again after 24 hours to remove the unattached cells and the contaminating fat droplets. Plating and expansion media used were Dulbecco's modified Eagle medium (DMEM – Sigma D 1152) supplemented with 10 % Fetal bovine serum

(Gibco) and 1% Penicillin – streptomycin (Gibco). Cultures were maintained at 37° C with 5% CO<sub>2</sub> and replenished twice a week. Once the ADSCs reached confluence of 80 to 90%, the cells were detached with 0.5 % Trypsin-EDTA (Gibco) and then replated . When sufficient cell numbers were attained, they were then evaluated for multilineage differentiation potential by driving them towards the osteogenic and adipogenic lineages.

#### **4.2.2 Differentiation into mesenchymal lineages**

##### **4.2.2.a. Osteogenic induction**

For inducing osteogenic differentiation, the cells were grown up to 80 to 90% confluence, trypsinised with 0.5 % Trypsin, replated into multiwell plates at a seeding density of 5000 cells per cm<sup>2</sup> and treated with osteogenic induction media. The cocktail was composed of 50 mM L-ascorbic acid-2-phosphate, 10mM β-glycerophosphate and 0.01 mM 1 α, 25 – dihydroxycholecalciferol in DMEM medium supplemented with 10% FBS. The induction was maintained for a minimum of 2 weeks, following which the cells were assayed for evidence of mineralization and osteogenic markers. For alizarin red staining the cells were plated in 24-well plates (NUNC), while for the immunohistochemistry the cells were plated into 48-well plates (NUNC). T-75 flasks (TPP) were used for plating cells required for RNA and protein extraction.

##### **4.2.2.b. Adipogenic Induction**

To induce adipogenesis, the cells were grown up to 80 to 90% confluence, harvested with 0.5 % Trypsin, replated into multiwell plates at a seeding density of 15,000 cells per cm<sup>2</sup>. The cells were treated with an induction cocktail composed of 0.5 mM isobutyl-



methylxanthine, 1 $\mu$ M dexamethasone, 10 $\mu$ M insulin and 200 $\mu$ M indomethacin in DMEM medium supplemented with 10% FBS. The induction was maintained for a minimum of 2 weeks, following which the cells were assayed for evidence of adipogenesis.

### **4.2.3 Histochemistry**

#### **4.2.3.a. Alizarin Red staining**

The cells were cultured in 24 well plates for 28 days and analyzed at day 14 and day 28. Prior to fixation, the samples were washed twice in PBS. Following fixation for 10 minutes with 10% buffered formalin, the cells were treated with Alizarin Red S working solution. The working solution was prepared by dissolving 2 g of Alizarin Red S powder in 100ml of distilled water. The pH of the working solution was then adjusted to 4.1 with 0.5% ammonium hydroxide. The wells were completely covered with the stain and left to stand for a period of 5 minutes. Subsequently the samples were washed with distilled water and observed under the microscope for presence of calcific nodules.

#### **4.2.3.b. Oil Red O staining**

The cells were cultured in 24 well plates for 28 days. The samples were washed with PBS, fixed with 10% neutral buffered formalin and then stained with working solution of 0.2% Oil Red O stain for 5 minutes. The excess stain was washed with deionized water and the nuclei counterstained with hematoxylin solution and observed under the microscope for the presence of neutral lipid vacuoles.

#### 4.2.4 Immunohistochemistry

Cells were seeded into 24 well plates at a density of 5000 cells per cm<sup>2</sup> and grown for period of 28 days in osteogenic induction media. As control, plain media without induction factors were used. The cells were analyzed at day 14 and day 28.

For immunostaining the cells were fixed with ice cold methanol at -20°C for 10 minutes. Non-specific antibody binding sites were blocked with 10 % goat serum at 25° C for 30 minutes. Subsequently the goat serum was removed and primary immunostaining was done for osteonectin, osteocalcin, collagen I and osteopontin by incubating at 4° C overnight (16 hours). Primary antibodies were used at the following concentration:

|   |   |        |
|---|---|--------|
| Rabbit anti human Collagen type 1 (Chemicon AB0745) | - | 1:500  |
| Rabbit anti human Osteopontin (Chemicon AB1870)     | - | 1:500  |
| Rabbit anti human Osteonectin (Chemicon AB1858)     | - | 1:1000 |
| Rabbit anti human Osteocalcin (Chemicon AB1857 )    | - | 1:500  |

Secondary antibody staining was performed with the HRP-conjugated anti-rabbit kit (DAKO Cytomation). The controls were blank specimens which were treated only with the antibody diluent, with no primary antibody being used. Immunostained specimens were counterstained with hematoxylin stain. All antibody dilution used were optimized earlier using Human fetal Osteoblast cell line as positive control and Human embryonic kidney cell line as negative control.

#### **4.2.5 RNA isolation and Real-time PCR analysis of ADSCs**

Cells were plated in 6 well plates in triplicates and grown in the presence of adipogenic or osteogenic induction media. Total RNA was harvested at time points 14 days and 28 days from these cells using RNeasy Kit (Qiagen). The concentration of the total RNA was measured with Nanodrop ND-100 spectrophotometer and stored at -80° C till further use.

##### **4.2.5.a. Reverse Transcription**

The purified total RNA obtained from the previous step was reverse transcribed into cDNA, using was done using RevertAid™ H-Minus MuLV Reverse Transcriptase enzyme (Fermentas). Briefly, about 100ng of total RNA was mixed with 800ng of oligodT (Proligo) and heated to 75° C for 8 minutes and chilled immediately on ice. A reaction mixture containing 1.0mM of dNTP, 20U of Ribolock™ Ribonuclease Inhibitor (Fermentas), 200U of RevertAid™ H-Minus MuLV Reverse Transcriptase enzyme and DEPC-treated water was added to the chilled mixture and incubated at 37° C for 1 hour. At the end, the enzyme was inactivated by heating at 70° C for 10 minutes. The samples were stored at -20° C till further use.

#### **4.2.5.b. Quantitative Real Time PCR**

The Quantitative Real-time polymerase chain reaction was done on Stratagene MX 3000P Real time PCR machine. Along with the cDNA samples, serial dilutions of the standards and non-template controls (NTC) were used for the PCR reactions. Quantitec SYBR™ Green PCR kit was used as the master mix for the real time PCR reactions.

Thermal cycling conditions for the reactions were: 95°C for 10 minutes, 45 cycles of 94°C for 30 seconds, 60°C for 45 seconds and 72°C for 30 seconds. The dissociation phase was carried out at 95°C for 1 second, 60°C for 30 seconds, slow ramp up to 95°C at 0.5°C per second with continuous measurement, 95°C for 10 seconds and finally brought down to 25°C. The primer sequences are shown in Table 4.1.

| <b>Adipogenic Genes</b>             | <b>Primer Sequence</b>                                       |
|-------------------------------------|--|
| Fatty Acid Binding Protein ( FABP ) | 5'-AACCTTAGATGGGGGTGTCC-3'<br>5'-GTGGAAGTGACGCCTTTCA-3'      |
| Leptin                              | 5'-TGACACCAAACCCTCATCA-3'<br>5'-ATGAAGTCCAAACCGGTGAC-3'      |
| Lipoprotein Lipase ( LPL)           | 5'-CCGGTTTATCAACTGGATGG-3'<br>5'-TGGATCGAGGCCAGTAATTC-3'     |
| <b>Osteogenic Genes</b>             | <b>Primer Sequence</b>                                       |
| Osteocalcin                         | 5'-TGTGGCATCCACGAAACTAC-3'<br>5'-GGAGCAATGATCTTGATCTTCA-3'   |
| Osteopontin                         | 5'-ACTACCATGAGAATTGCAGTGA-3'<br>5'-TCCTCAGAACTTCCAGAATCAG-3' |
| Osteonectin                         | 5'-CCACCTGGACTACATCGG-3'<br>5'-TCCTCATCCCTCTCATAACAG-3'      |
| Runx-2                              | 5'-TCTTCCCAAAGCCAGAGTG-3'<br>5'-CATGGGAAACTGATAGGATCC-3'     |

**Table 4.1** – Primer sequence of genes used for real time PCR

#### 4.2.5.c Standard Preparation

The standards for real time PCR was prepared from the products of an end point PCR. Using the above primers, the amplified PCR products of an end point PCR was run on a 2% agarose gel. The bands on the gel were visualized under UV light, the amplified products cut from the gel and purified using a silica column based DNA extraction kit (vCell Science) as per the manufacturer's protocols. The DNA was eluted from the silica column and the quantity of the recovered DNA measured on a Nanodrop ND-1000 spectrophotometer. The copy numbers of the gene in this given volume could be calculated using the combination of DNA concentration, molecular weight of the amplicon and Avagadro's constant, as per the formula:

$$\text{Copy number} = \frac{\text{mass}}{\sum n_N M_N} \times A_v$$

$n_N$  - number of each dNTP expected in PCR product.

$M_N$  - molecular weight of each mole of dNTP

$mass$  - mass of PCR product quantified from spectroscopy.

$A_v$  - Avagadro's constant =  $6.02 \times 10^{23}$

For each set of genes tested, the samples were run in triplicates and the data was analyzed by student's two tailed paired T-test. The significance was set at a p-value of less than 0.05.

#### **4.2.6 Western Blot Analysis for Osteogenic proteins**

Cells were plated into 6 well plates and grown in the presence of osteogenic medium for at total period of 28 days. Uninduced samples were used as the control. Following induction, the cells were harvested at 14 days and 28 days. The cells were lysed in Triple detergent lysis buffer with added Protease Inhibitor (Sigma). The buffer's components were:

50mM Tris-HCl (pH 8.0)

150mM NaCl

0.1 % SDS

1 % NP – 40

0.5 % w/v sodium deoxycholate

Subsequently, the lysed specimen was centrifuged at 14,000 rpm for 20 minutes and the supernatant collected. To concentrate the protein samples, they were loaded onto Nanosep™ Centrifuge tubes (Pall Inc.) and desalted using distilled water. The total protein extracted was quantified using a micro BCA kit (Pierce).

Following this, about 50 µg of the protein samples were treated with 6 X loading at 90° C for about 10 minutes and loaded onto a 10% SDS gel along with Dual color Protein ladder (Bio-Rad). The loaded gel was run at 150 V till the dye front was washed away from the edge of the gel plate. The gel was subsequently transferred onto a PVDF membrane, using transfer parameters of 90 V and 600mA for about 1 hour. The transfer was verified by staining the blots with Ponceau-S stain (Pierce).

For all samples, the blots were blocked with 1% milk for half an hour at room temperature and incubation with the primary antibody was carried at 4° C, overnight (16 hours). The primary antibody concentrations used were:

|   |   |         |
|---|---|---------|
| Rabbit anti human Osteopontin (Abcam, Ab8448)           | - | 1:1,000 |
| Rabbit anti human Osteonectin (Santacruz, SC25574)      | - | 1:1,000 |
| Rabbit anti human Osteocalcin (Santacruz, SC30044)      | - | 1:1,000 |
| Rabbit anti human $\beta$ -actin (Delta Biolabs, DB070) | - | 1:2,000 |

The secondary antibody treatment was done with anti-Rabbit antibody conjugated to HRP (Horse radish preoxidase) enzyme, raised in goat (Zymed, 62-6120) and was used at a concentration of 1:15,000. The blots were subsequently treated with Luminol HRP substrate (Pierce) for 10 minutes and visualized in Versadoc Imaging station (Biorad).



## 4.3 RESULTS

### 4.3.1 ADSC morphology

Freshly plated ADSCs demonstrated varying morphology. Initially the ADSCs had a polygonal morphology (Fig 4.1A). After 3 weeks of culture, the morphology changed and the cells became predominantly spindle shaped (Fig 4.1B). Thus it could be said that the freshly acquired ADSCs constitute a population of heterogeneous cells, which change their morphology and become predominantly spindle shaped.

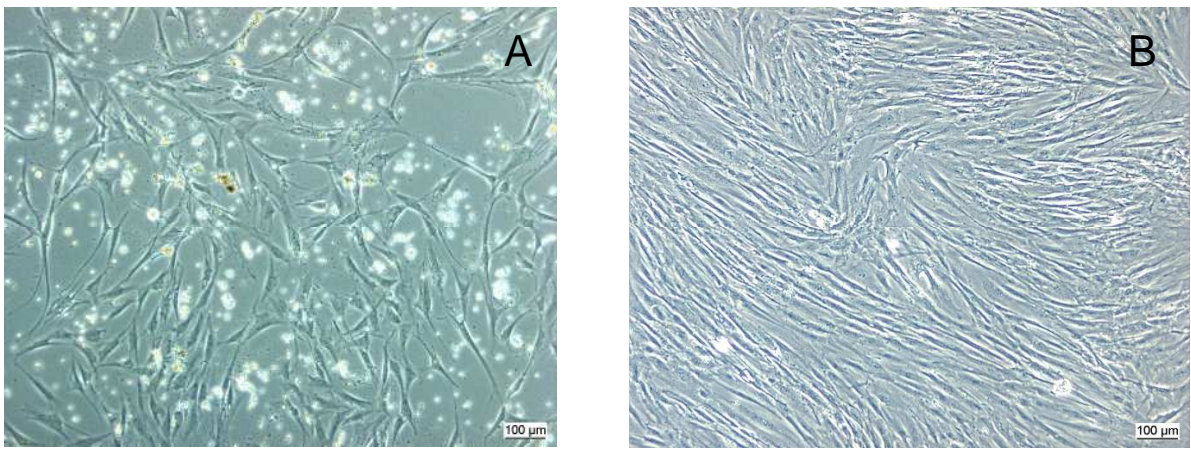


**Fig 4.1 - Morphology of ADSCs plated on tissue culture plastic.** The initial morphology which was flat and polygonal (Fig 4.1A) changed to spindle shaped on continued culture (Fig 4.1B)

### 4.3.2 Histological evidence of osteogenesis

Alizarin Red staining of the ADSCs grown in osteogenic media revealed foci of mineralization (Fig 4.2B, the areas stained in dark red), when compared to the control ADSCs without any osteogenic induction (Fig 4.2A)

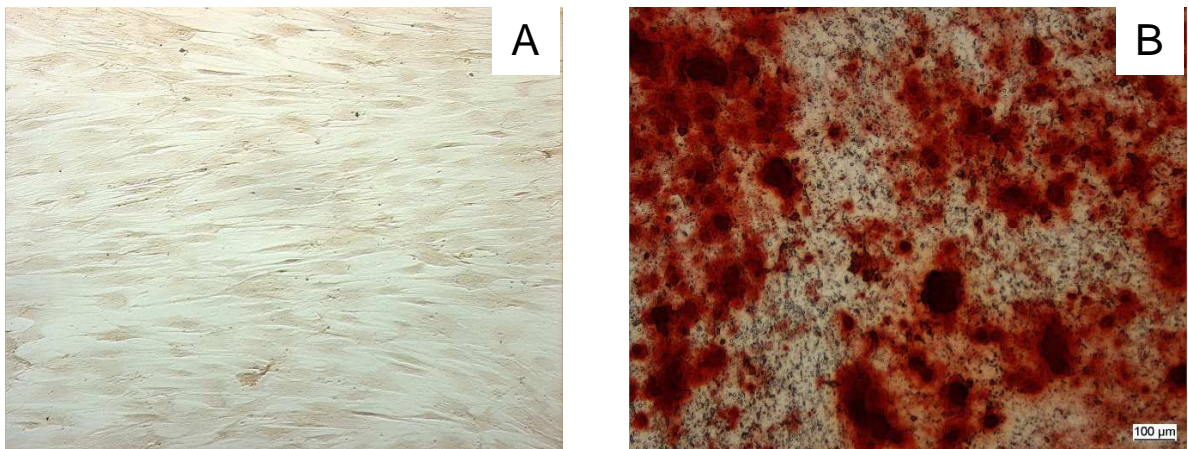


**Fig 4.2 - Alizarin Red staining of ADSC.** The uninduced samples (Fig 4.2A) do not take up any stain. Intense foci of mineralization seen in the induced samples (Fig 4.2B)

### 4.3.3 Immunohistochemistry for osteogenic makers

Immunostaining showed that ADSCs expressed markers of osteogenesis like collagen I, osteocalcin, osteonectin and osteopontin as early as 14 days after induction and by 28 days there was marked expression of the same (Fig 4.3B,D,F,H). Control samples, which were uninduced, failed to express these markers on immunostaining (Fig 4.3A,C,E,G).

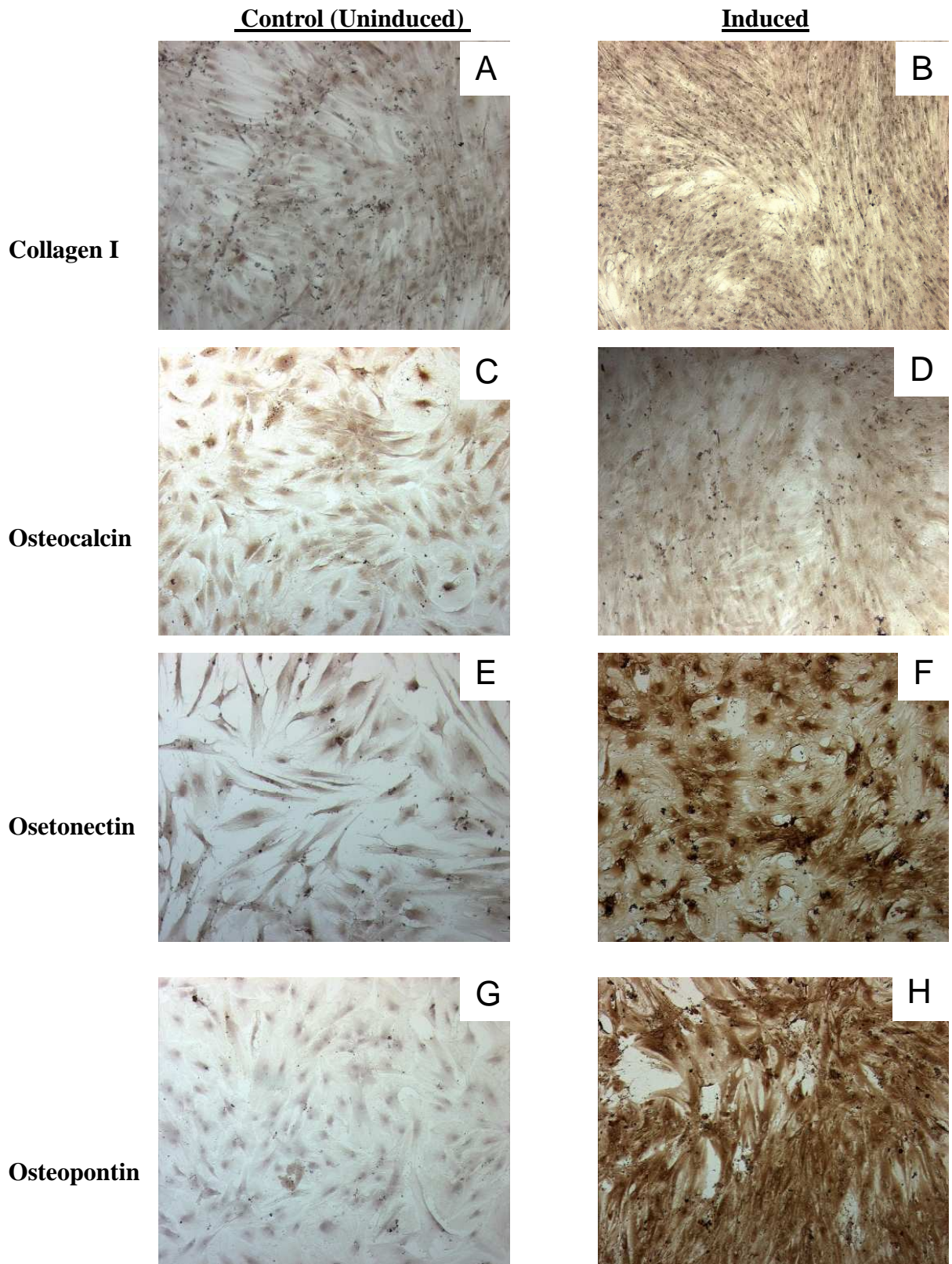


**Fig 4.3-Immunohistochemistry of osteogenic markers at 28 days. Increased expression for the respective markers seen in the induced groups at (B,D,E,F) compared to the uninduced group (A,C,E,G).**

#### 4.3.4 Adipogenic potential of the ADSCs

When ADSCs are grown in adipogenic media, they began forming lipid droplets after 2 weeks of induction (Fig 4.4A) and increased significantly by day 28 (Fig 4.4B). Uninduced ADSCs did not form lipid droplets by this time (figures not shown), demonstrating that the ADSCs retained their adipogenic potential and when given the right set of stimuli, they could commit themselves to this lineage.

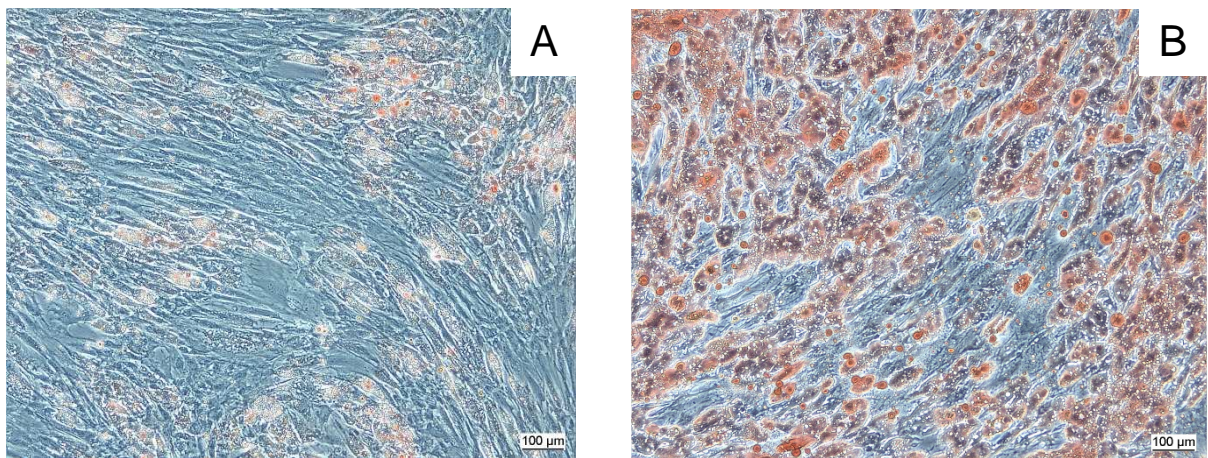


**Fig 4.4 - Oil Red O stain for fat vacuoles.** Fat vacuoles could be detected as early as day 14 in the induced samples (Fig 4.4A) and increased all the way upto day 28 (Fig 4.4B)

#### 4.3.5 Real time-PCR analysis of gene expression

##### 4.3.5.a Adipogenic Genes

Real time PCR analysis of the total RNA extracted from ADSCs subjected to adipogenic induction revealed that these populations of cells retained their native potential and were capable of differentiation into adipocytes under the influence of adipogenic stimuli. Compared to the uninduced control samples, the induced samples were the only ones showing evidence of adipogenesis. The three genes that were analyzed for evidence of

adipogenesis were: Fatty acid binding protein (FABP), Leptin and Lipoprotein Lipase (LPL).

#### 4.3.5.b FABP expression

All the three ADSC samples showed increased expression of FABP gene in the induced samples, while in the uninduced samples hardly any expression was seen (Fig 4.5A and B).

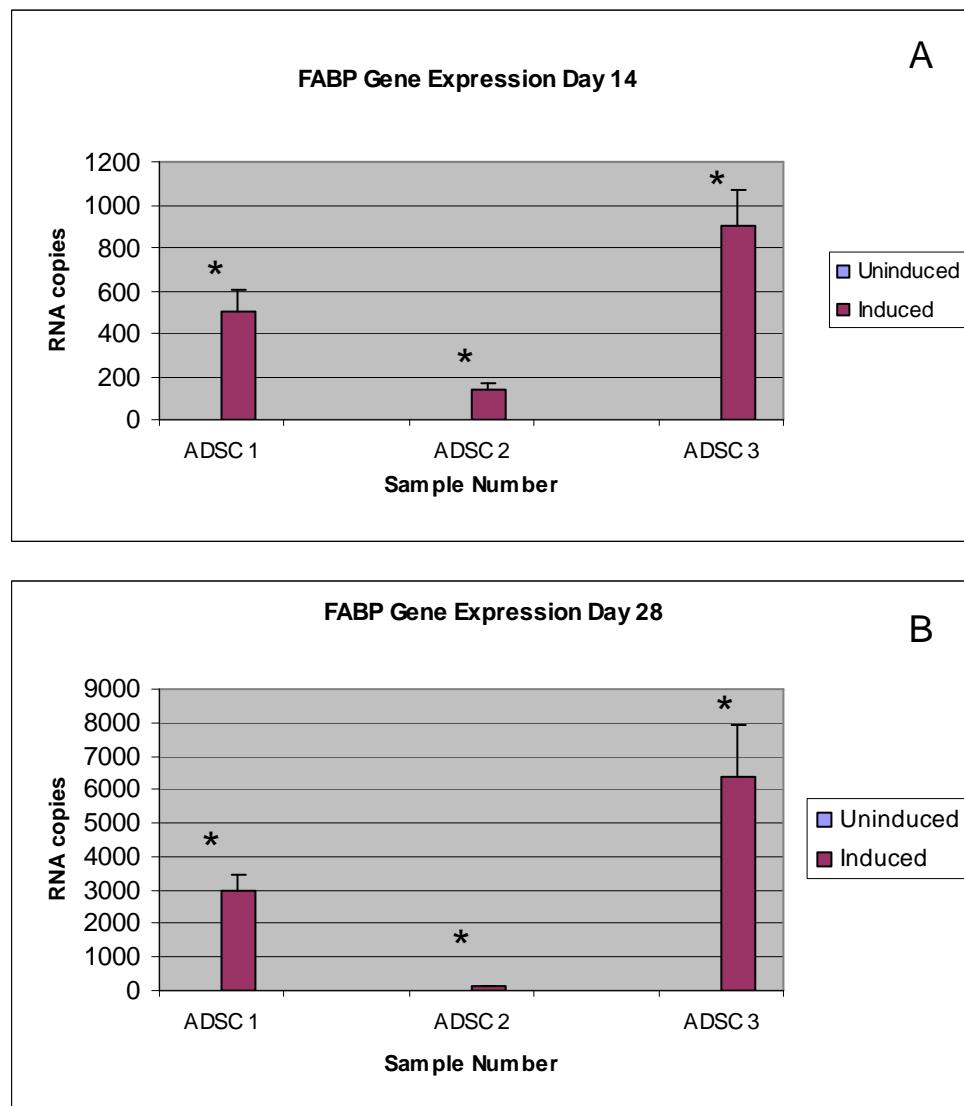


**Fig 4.5 - FABP expression in ADSCs following adipogenic induction.** The expression in day 14 samples (Fig 4.5A) and day 28 samples (Fig 4.5B) were similar in pattern, with increased expression seen in the induced samples.

### 4.3.5.c LPL Expression

Similar to the expression pattern seen with FABP gene, LPL expression was also found to be more in the induced samples, with hardly any expression seen in the uninduced. The gene copies in the day 28 samples were much higher, when compared to the same in the day 14 samples (Fig 4.6A and B).

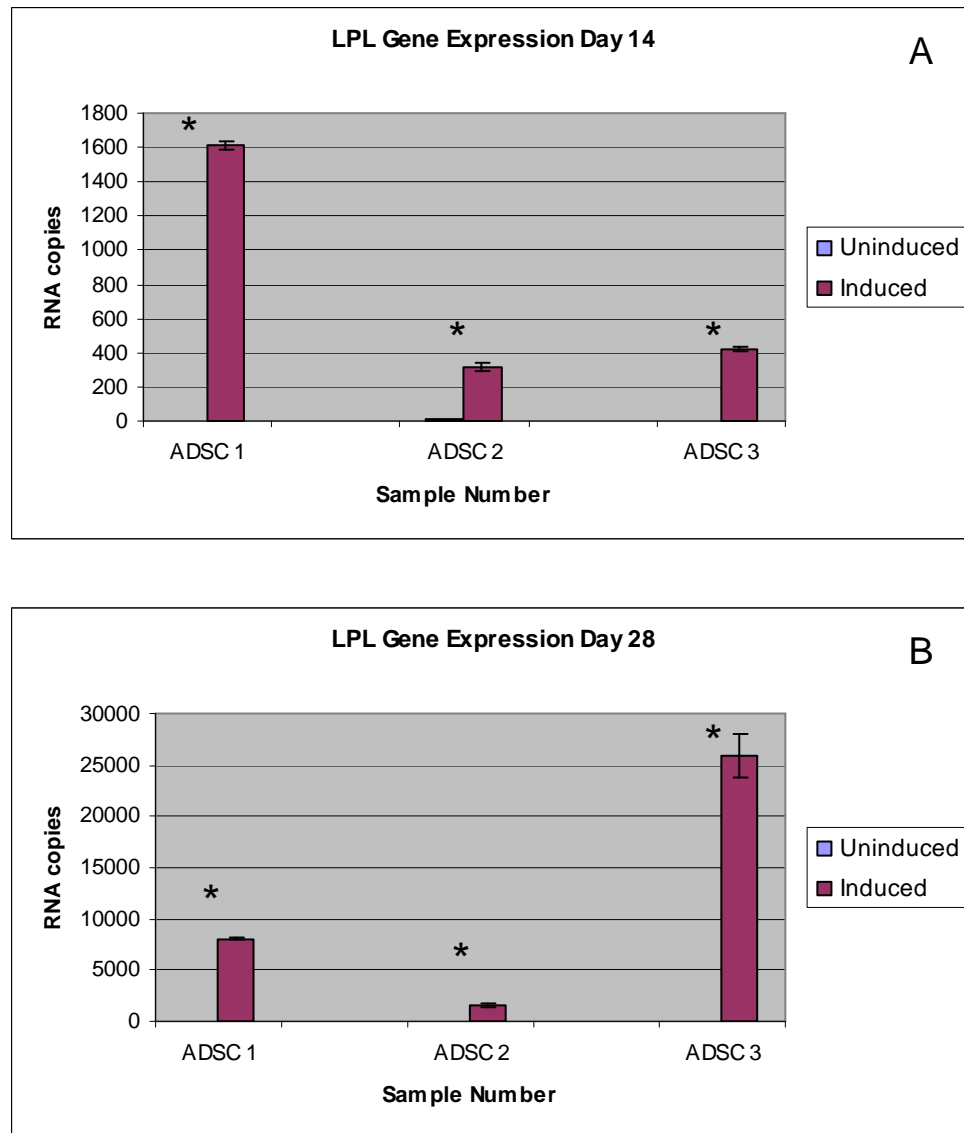


**Fig 4.6 – LPL expression in ADSCs following adipogenic induction.** The expression in day 14 samples (Fig 4.6A) and day 28 samples (Fig 4.6B) were similar in pattern, with a significantly increased expression seen in the induced samples

#### 4.3.5.d Leptin Expression

The leptin expression pattern was different from the above two. Leptin expression was not seen in the day 14 samples in both the induced and uninduced groups (data not shown). However expression was seen in the day 28 samples (Fig 4.7). There was significant difference in the expression levels between the induced and uninduced categories of two of the samples.

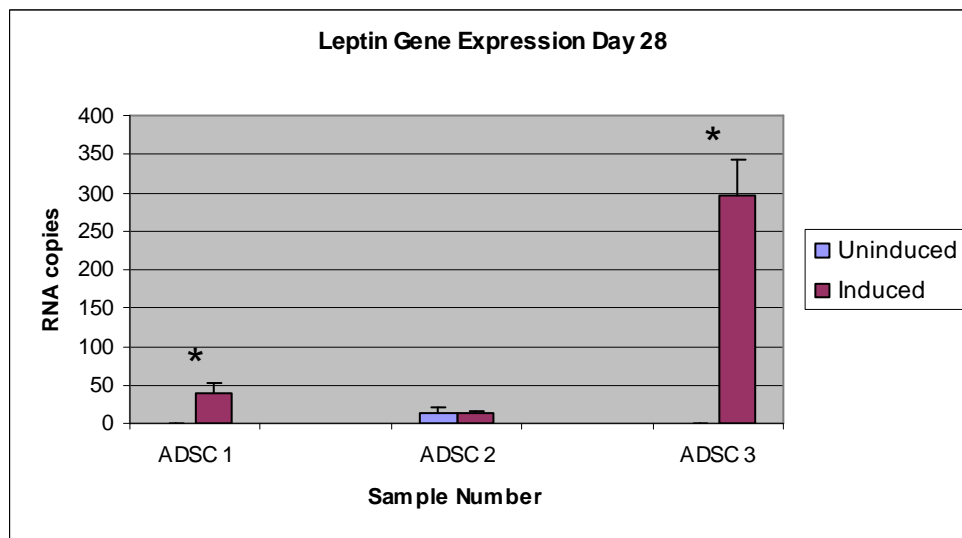


**Fig 4.7 – Leptin expression in ADSCs** following adipogenic induction at day 28. The expressions in day 14 samples were not detectable (data not shown).

#### **4.3.6 Osteogenic Genes**

Real time PCR analysis of the total RNA of the ADSCs after osteogenic induction showed that these population of cells were able to express markers of osteogenesis to varying extents.

##### **4.3.6.a Osteocalcin expression**

Osteocalcin has been considered as one of the most specific markers for osteogenic differentiation (Ducy P et al., 2000). In the day 14 samples tested, the levels of osteocalcin in the osteo-induced ADSC samples were found to be much lower than that of the induced (Fig 4.8A). However, by day 28 the exact opposite pattern was seen (Fig 4.8B). By 28 days of induction, the osteo-induced ADSCs showed a significantly higher expression of osteocalcin gene (p-value < 0.05).



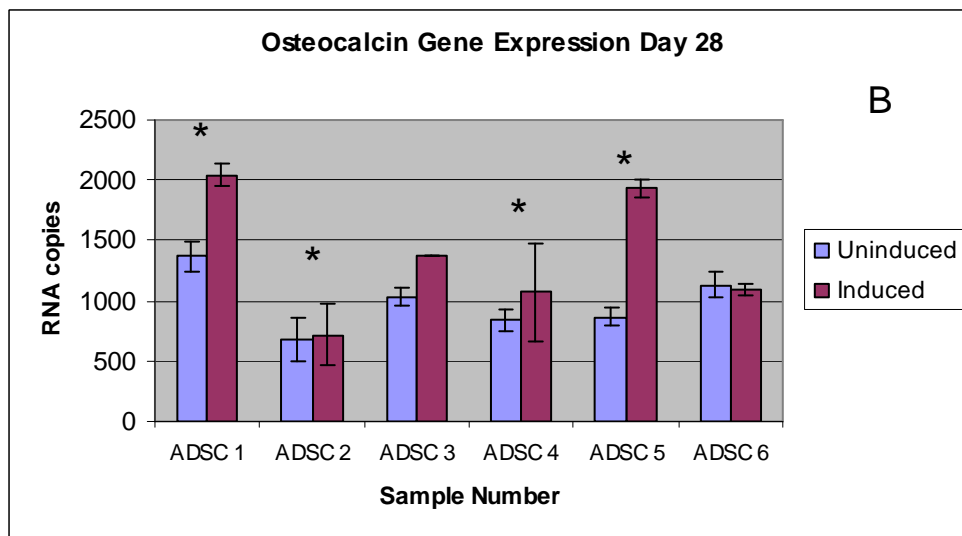
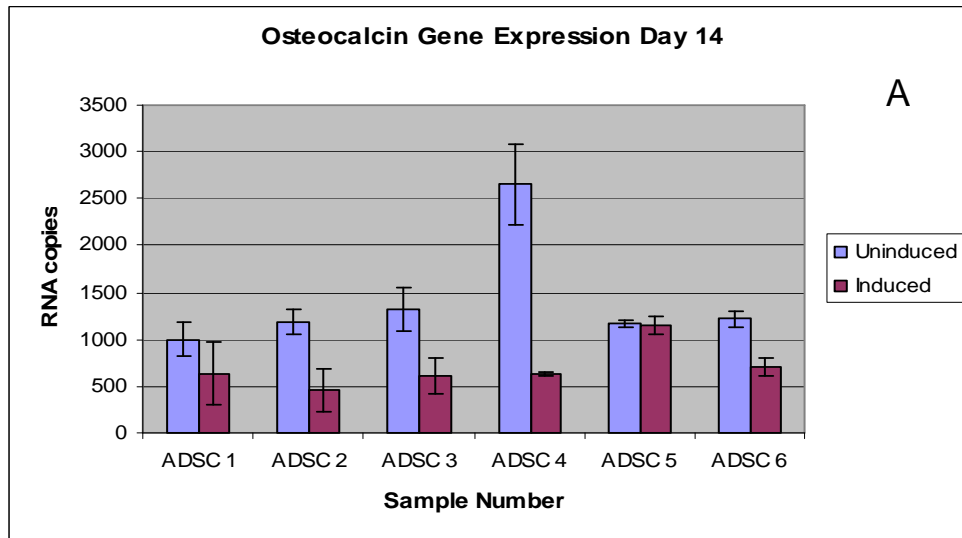


**Fig 4.8 – Osteocalcin expression.** The levels of the gene were quite low in the day 14 samples (Fig 4.8A). However majority of the samples showed a significantly increased expression by day 28 (Fig 4.8B)

#### 4.3.6.b Runx2 expression

Runx2 expression pattern were similar to that seen in osteocalcin. While in the day 14 samples, the expression of the gene was very low (Fig 2.9A), by 28 days of induction the induced samples started showing significantly higher levels of expression, when compared to the uninduced samples (Fig 4.9B, p-value < 0.05).

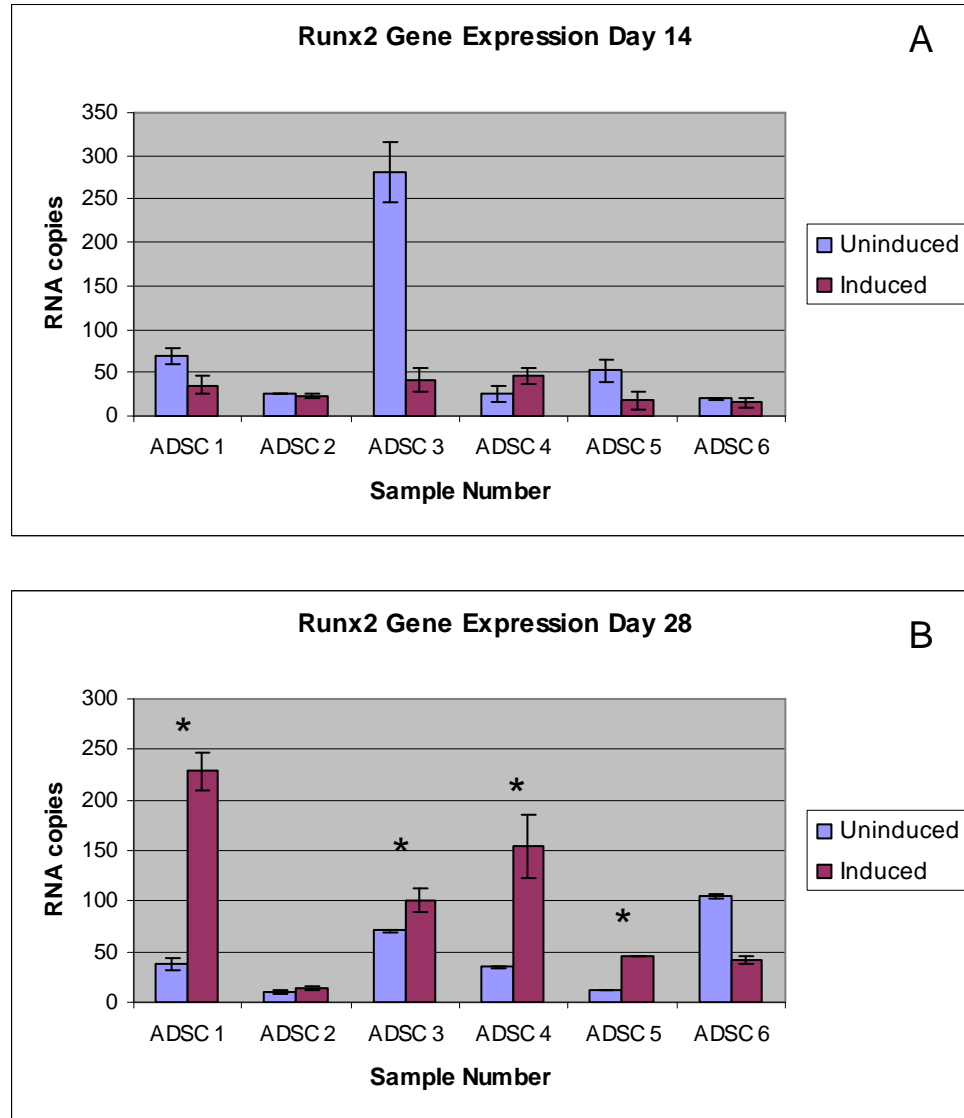


**Fig 4.9 – Runx2 expression.** The levels of the gene were quite low in the day 14 induced samples (Fig 4.9A). However, by day 28 a significantly increased expression was seen in the induced samples showed a significantly increased expression by day 28 (Fig 4.9B)

#### 4.3.6.c Osteopontin and Osteonectin expression

The expression of these non-specific osteogenic markers were highly variable, with some of the induced samples having a much lower levels of expression when compared to the uninduced samples (data not shown). However by day 28, the samples showed a much higher level of expression of osteopontin (Fig 4.10A) and osteonectin (Fig 4.10B) when compared to the day 14 groups.

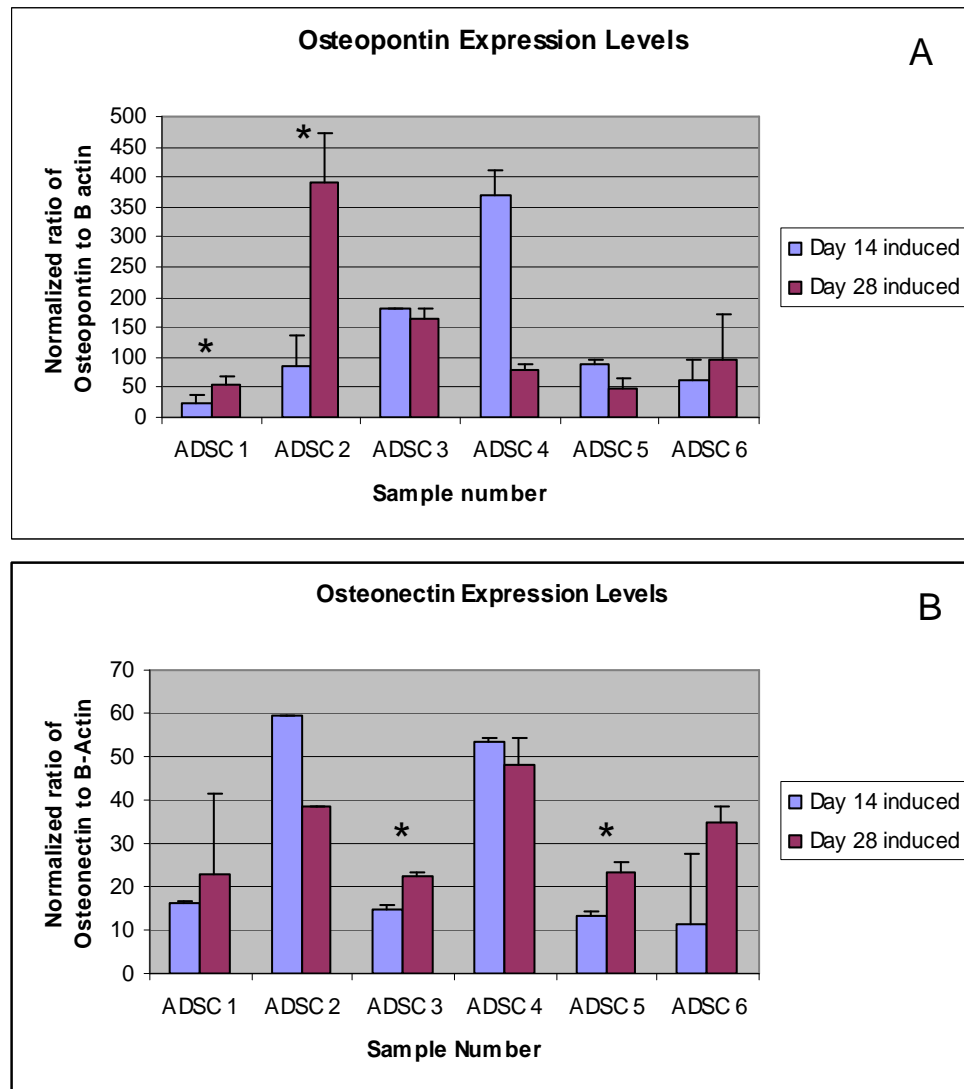
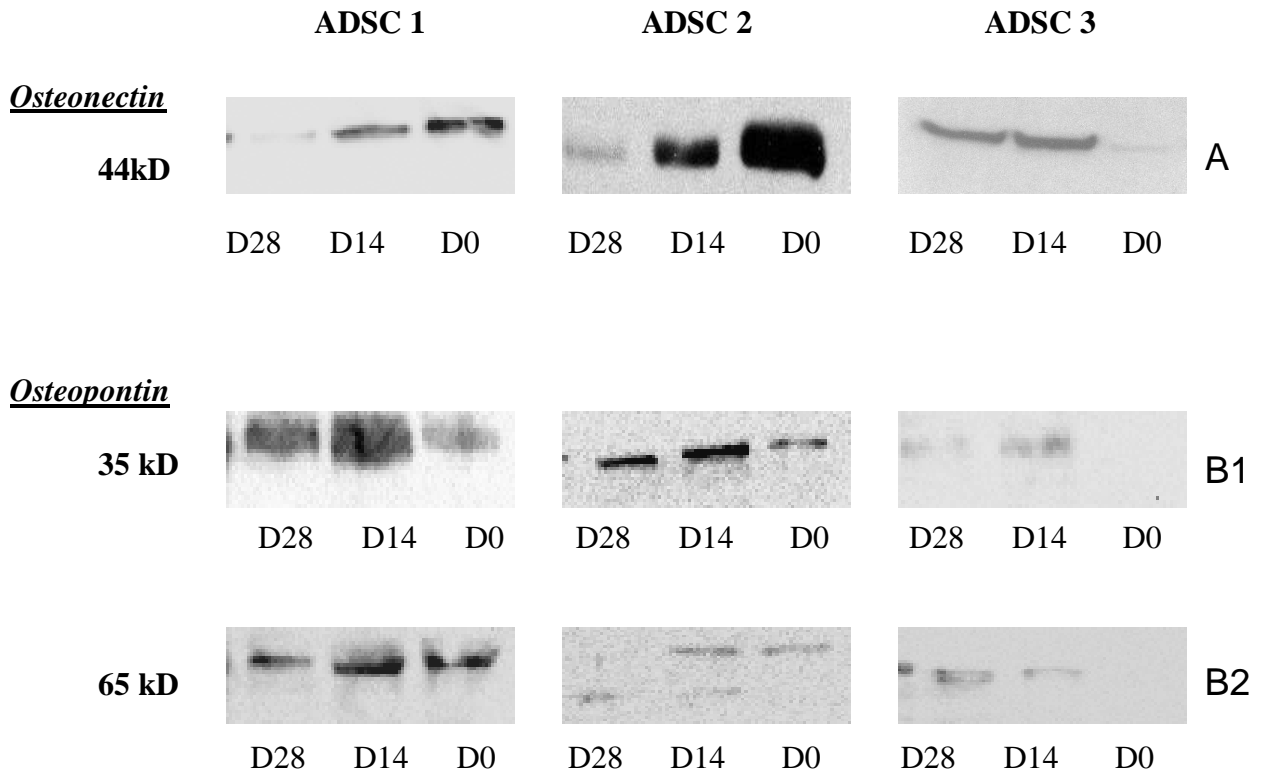


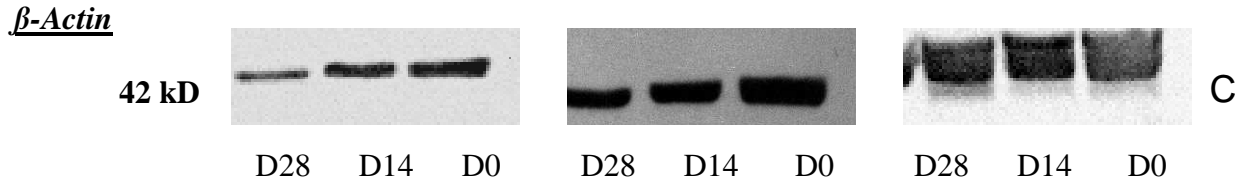
**Fig 4.10 – Osteopontin and osteonectin expression.** In a few of the samples, the expression of osteopontin was much higher at 28 days of induction (Fig 4.10A) when compared to the day 14 samples. A similar profile was seen with osteonectin expression (Fig 4.10B)

### 4.3.7 Western blot for osteogenic markers

Western blot was done for osteonectin (Fig 4.11A), osteopontin (Fig 4.11B) and  $\beta$ -actin (Fig 4.11C) proteins in all of the samples. A few of them showed an increasing trend in protein production from day 0 to day 28. However, this phenomenon could not be uniformly seen in all the samples. In some of the samples these proteins could be detected as early as day 0. Western blots were also done for osteocalcin protein, but due to inconsistencies in the molecular weight of the protein obtained, the data has not been shown. Osteonectin was seen at a molecular weight of 44 kD. Osteopontin has been to know have two major isoforms; they were detected at 35 kD and 65 kD.

Positive controls used for the experiments were hFOBs (human Foetal Osteoblast cell lines)





*Control (hFOBs cell line)*

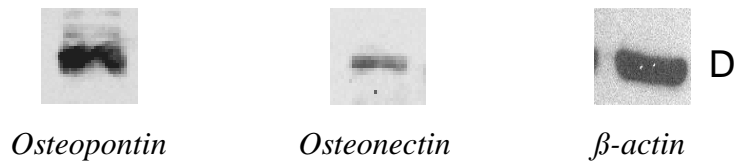


**Fig 4.11 – Western blots for osteogenic markers.** Osteonectin and osteopontin expression (Fig 4.11 A and B) show a variable expression with time. Fig 4.11 B1 and B2 show the two different isoforms of osteopontin obtained. As a control  $\beta$ -actin (Fig 4.11 C) and hFOBs cell line (Fig 4.11 D) were used

**4.4 DISCUSSION**

Adipose tissue is currently being researched as an excellent source of precursor cells for the purpose of tissue regeneration. Though it is quite often thought of as a heterogeneous cell population, it is still possible to isolate precursor cells with multilineage differentiation potential. From the initial analysis of the basic characteristics of the cells isolated from the lipoaspirates, it could be said that these population of cells indeed possess precursor cell like properties.

The cells when plated initially possessed a polygonal morphology, but with progression of culture and passages they tend to acquire a spindle shape. This is in accordance with literature evidence of the changing morphology of ADSCs when grown in culture (Zuk et al., 2000).

These cells when exposed to osteogenic induction cocktail tend to exhibit the property of lineage commitment. Under the influence of these factors, the cell began to exhibit light microscopic features of mineralization. Alizarin red stain revealed foci of calcific nodules in the induced samples, whereas no such foci were seen in the uninduced ones (Fig 1.1). Similarly, immunohistochemistry for bone markers like osteocalcin, osteonectin and osteopontin revealed that the induced cells showed a considerably greater expression of these when compared to the uninduced.

To corroborate these findings, the real time PCR analysis done on ADSCs showed that those groups exposed to osteogenic cocktail tend to express a higher level of markers like osteocalcin and Runx2, although from these experiments the same could not be said of the other two markers, osteopontin and osteonectin.

Osteocalcin has been considered as an important and specific marker for osteogenic lineage commitment (Ducy P. et al., 2000). It is one of the most abundant of the non-collagenous proteins in bone, having calcium binding properties (Hauschka, P et al., 1989). The major role of this protein is in preventing excessive calcium deposition in bone and is therefore considered a negative regulator of mineralization (Ducy P. et al., 2000). However, it is a very specific marker for osteogenic differentiation and is highly expressed during the early stages and the much later stages of bone formation. Similarly, Runx2, which is quite often considered the “master switch” triggering osteogenesis, is also a very specific marker for this process and acts upstream of osteocalcin (Banerjee C et

al., 1997). Not all the six samples in this study were able to express significant amounts of these proteins.

Osteopontin and osteonectin have been traditionally considered as markers of osteogenesis, though by themselves, they are not very specific for osteogenesis as compared to osteocalcin or Runx2 (Dragoo JL et al., 2003 ; Ogawa R et al., 2004 ; Rodan GA et al., 1999 ; Heinegård D et al., 1989). Osteopontin is a highly acidic protein that is predominantly expressed in the early stages of bone formation, but can be found in a host of other tissues (Butler WT., 1989). There are two major isoforms of this protein. We were able to detect the two isoforms at 65 kD and 35 kD. Osteonectin also enjoys a similar profile and is found during the early stages of bone formation, where it plays a role in nucleation of the apatite crystals (Fujisawa R. et al., 1991).

The above results show considerable variation in the expression pattern of different genes and proteins over the period of study. Runx2 and osteocalcin expression was fairly steady and constant across the experimental groups, with 4 out of 6 samples showing an elevated expression of these markers in the induced group. However, such a profile was not seen in the expression pattern of osteopontin or osteonectin. Similar variations in gene expression patterns have been previously reported in a variety of other studies involving human bone marrow MSCs. Work done by Frank O. et al., showed that the expression of osteogenic markers like alkaline phosphatase, osteocalcin , cbfa1 (i.e. Runx2) by bone marrow MSCs exposed to osteogenic induction stimuli were inconsistent across samples (Frank O et al., 2002). Such variation have been reported by other groups working on bone marrow MSCs (Jaiswal N et al., 1997) and most recently shown in human bone

marrow MSCs of around 19 different donors across varying age groups (Siddappa R et al., 2007).

Several reasons could lie such variations, such as differences in the composition of the initial aspirate and population of the precursor cells, differential sampling techniques by physicians which could result in cell populations of varying heterogeneity, functional differences in the osteogenic potential of the MSCs and even the physiological status of the patients from whom the samples were isolated (Siddappa R et al., 2007). Such an inter donor variability could also be operational when ADSCs are collected and characterized. Thus, the osteogenic potential of one set of ADSCs might be different from another. The protein expression patterns of osteopontin and osteonectin were studied and were also found to be highly variable. While in a few samples there was a consistently increasing expression pattern from day 0 to day 28 induced groups, a few of the samples showed a constant expression pattern from the beginning itself. This again, could be attributed to sample variability and also the relative non-specificity of these two markers in osteogenesis.

Osteogenic differentiation of ADSCs is an area of research which is being extensively pursued in several labs. On the one hand the intricate molecular mechanisms that governs this process in ADSCs is being evaluated (Luzi E et al., 2008), while on the other hand the same phenomenon is being studied on three dimensional surfaces (Lee JH et al., 2008).



## **4.5 CONCLUSION**

From this study, it was possible to isolate an adherent population of cells (ADSCs) from the lipoaspirate of donors. These cells are have the ability to differentiate into two different lineages and could therefore be considered as being multipotent. These ADSCs showed evidence of osteogenesis when exposed to osteogenic stimuli.

Histology and immunohistochemistry showed evidence of osteogenesis like calcific nodules and extracellular matrix deposits respectively. These findings were corroborated by similar results with real time PCR and western blot analysis. However, the results of real time and western blots were not uniform across all the donor samples.

Therefore, ADSCs obtained from the adipose tissue could be considered as a sizeable depot of MSCs having multipotent nature and for use in tissue regeneration in orthopedic applications.

## **Chapter 5**

### **RNA INTERFERENCE (RNAi) SILENCING OF ATF5 IN ADSCs**

#### **5.1 INTRODUCTION**

ADSCs are presently being investigated as candidate cells for use in bone tissue regeneration, but the events that dictate the process of osteogenic differentiation in these cells are far from being precisely outlined. A proper understanding of the mechanisms that govern the process of osteogenesis in bone cells would give us an insight into how similar events occur in non-osteogenic precursor cells. The principle factors that govern osteogenic differentiation of precursor cells are Cbfa1 / Runx-2 (Ducy P et al., 1997). This transcription factor regulates the activation of lineage specific markers like osteocalcin, osteopontin and collagen I (Ducy P., 2000) While much of the work done has been on osteoblast cells, the factors that govern similar fates in non-osteogenic precursor cells have not been clearly elucidated. Literature is abounding with evidence of induction factors being capable of driving non-osteoblast precursor cells towards the osteogenic lineage. Zuk PA et al. have shown the ability of adipose tissue stromal cells to differentiate towards osteogenic lineage under the influence of a cocktail of chemical substances. Osteogenic differentiation has been demonstrated in hematopoietic precursor cells (Kondo M et al., 2003) and in mesenchymal precursor cells isolated from the peripheral blood (Villaron EM et al., 2004).

Work done by Yang et al has demonstrated the existence of a unique transcription factor, Activating transcription factor 4 (ATF4), which can induce the expression of the osteoblast-specific gene, osteocalcin, in non-osteoblast cell lines in vitro. They were able to show that ATF4 accumulation in osteoblasts is mediated by a post-translational ubiquitination process, which normally degrades this factor in other cell lines. Subsequently it was shown that ATF4 indeed interacts with the master transcription factor, Cbfa1/ Rux2 through its leucine zipper domain to stimulate osteocalcin expression (Xiao G et al., 2005). Non-osteoblast cell lines which were co-expressed with ATF4 and Runx2 demonstrated an increased osteocalcin mRNA expression. Therefore, it might be possible that this transcription factor might play a significant role in ADSCs as well.

The whole genome transcriptome analysis of ADSCs (PhD work of Leong TWD) done in our lab, had shown that when these cells are exposed to osteogenic stimuli, several genes undergo a variable fold change. A total of twenty patient samples were put through the process of osteogenic induction and the gene expression was performed using Affymetrix Gene chips. Looking for genes that underwent a significant fold change in expression revealed that one particular gene, ATF5 was consistently down regulated in nineteen out of the twenty samples analyzed. ATF5, properly known as Activating Transcription Factor 5, belongs to the family of cAMP binding elements having a leucine zipper motif (Hai T et al., 2001).

The consistent down regulation of this gene in ADSCs observed from the gene chip data, was further validated by using real time PCR (PhD thesis of Leong TWD). These data

indicate that ATF5 could possibly have a role during osteogenic differentiation in ADSCs, whereby suppression of ATF5 is a necessary or accompanying event during osteogenic differentiation. It might be hypothesized that ATF5 acts to repress osteogenic differentiation in ADSCs and exposure to an osteo-induction cocktail, circumvents this repression to bring about commitment towards the osteogenic lineage. A similar role for ATF5 has been proven by Angelastro JM et al (2005) in neural precursor cells, where it was shown that a down regulation of ATF5 is a prerequisite for the maturation of these cells into astrocytes and oligodendrocytes.

As a continuation of this work, we analyzed the expression of ATF4 gene, which as previously mentioned, is an important regulator of osteogenic differentiation in non-osteoblast cell types. Ten of the ADSC samples in the above study were put through a 28 day osteoinduction period and the RNA isolated for ATF4 expression analysis.

A primary step towards understanding the observed phenomenon of a consistent down regulation of the ATF5 gene would be to see how the process of osteogenesis in ADSCs would be affected when ATF5 gene is not expressed. If ATF5 expression does affect osteogenesis, when the expression of this gene is repressed, one would see a reciprocal expression of the classical markers of osteogenesis. Gene silencing of ATF5 should be able to trigger or derepress downstream events which are under the influence of ATF5. In order to do study this, we decided to block the mRNA expression of ATF5 in ADSCs by specific small interference RNA (siRNA) sequences to ATF5, delivered to the cells using lipophilic carriers.

RNA interference, otherwise known as RNAi, is a naturally occurring phenomenon which is an effective form of post-translational sequence specific gene suppression (Fire A et al., 1998). In nature, RNA interference is mediated by short double-stranded RNA molecules which are processed into 20 to 23 base long RNAs called siRNAs, and then form part of the RNA-induced silencing complex (RISC) triggering a nuclease that degrades the target RNA (Kurreck J., 2003). In vivo, this type of gene silencing is highly specific for the target mRNA sequences, with minimal off-target effects seen (Chi JT et al., 2003); however some sequences may have diverse and unwarranted effects. Commercially available siRNA sequences used for gene silencing have been chosen after a stringent evaluation of several target sites within a particular gene, following which the sequences that require that lowest concentration for gene silencing and having minimal off-target effects are selected (Vickers TA et al., 2003). Some of them have been chemically modified by introducing synthetic nucleotides, so as to stabilize their structure and function in cell culture and in vivo (Amarzguioui M et al., 2003). RNAi technology is also being widely experimented as a form of nucleic acid-based therapies, as targeted gene silencing could be a perfect tool for identifying gene function and use as a therapeutic agent (Scherer L et al., 2004).

Following the silencing of ATF5 in them, the ADSCs were exposed to two different concentrations of induction cocktails, a sub-optimal concentration (0.1X) and the optimal concentration (1X), for a period of five days, during which cells were harvested at three different points, the total RNA extracted and analyzed for the expression of ATF5, osteocalcin and ATF4 genes. Osteocalcin, being one of the earliest and most specific

markers for osteogenesis, would seem like the most appropriate gene to undergo variable expression during these initial stages of osteogenic differentiation. Cells that travel down the osteogenic lineage would show an elevated expression of osteocalcin. On the contrary, cells that do not move along this lineage would not be showing an increased expression. ATF4 on the other has been considered to be one of the genes that influence osteogenic differentiation in non-bone cells (Yang X et al., 2004a). Its structural homology with ATF5 could also imply that these two sets of transcription factors may interact during the process of osteogenic differentiation in ADSCs. Therefore, the expression pattern for ATF4 could give an indication of the extent of interplay between ATF4 and ATF5 in ADSCs subjected to osteogenic differentiation. A short time frame of 5 days for the study was chosen based on the presumption that ATF5 would have its role during the early stages of differentiation, when ADSCs would be committing themselves to the osteogenic lineage.

Traditionally the optimal expression of markers for osteogenesis occurs at an induction factor concentration of 1X. The logic of using the 0.1X concentration along with the 1X concentration were to see if any changes in osteocalcin expression could be picked up even at these sub-optimal induction conditions.

If ATF5 indeed suppresses osteogenic differentiation in ADSCs, silencing of ATF5 gene should be able to promote osteogenesis and hence an early expression of osteocalcin would be seen; while in the non-silenced control groups, such an effect would not be seen. Also if ATF4 and ATF5 have a reciprocal role in modulating osteogenic

differentiation, one would expect to see a rise in ATF4 expression when the ATF5 gene is silenced.

## **5.2 MATERIALS AND METHODS**

### **5.2.1 Cell Culture**

ADSCs were cultured as previously mentioned. Once the cells reached confluence, they were trypsinised and counted. The cells were subsequently plated in 6-well plates at a density of 100,000 cells per well in 2.5ml of plating medium. When the cells reached a confluence of 50 to 70 %, they were transfected.

### **5.2.2 Transfection of ATF5 Stealth™ RNAi into ADSCs**

Transfection of the ATF5 Stealth™ RNAi was done based on the protocols provided by the company on their website ([www.invitrogen.com](http://www.invitrogen.com)). The RNAi was delivered into the cells using Lipofectamine™ RNAiMAX Transfection Reagent (Invitrogen). For transfecting MSCs, the protocol of Forward Transfection was used, whereby Lipofectamine – RNAi complexes were prepared and added to cells plated the previous day. Briefly about 100,000 ADSCs were plated into each well of a 6-well plate in about 2500 µl of DMEM without serum or antibiotics. The cells were 30% to 50% confluent when transfected.

The following day, the RNAi duplex-Lipofectamine™ RNAiMAX were prepared. Initially about 30 pmol of the RNAi duplex was diluted in about 250 µl of Opti-MEM® I Reduced Serum Medium (Invitrogen) without any added serum and mixed gently in a 50

ml Falcon tube. In a separate tube, about 5  $\mu$ l of the Lipofectamine<sup>TM</sup> RNAiMAX Reagent was diluted in 250  $\mu$ l of Opti-MEM<sup>®</sup> I Reduced Serum Medium and mixed. The contents of both the tubes were mixed gently and incubated at room temperature for 20 minutes. At the end of this time, the mixture was added to each well, giving a final volume of 3000  $\mu$ l and a final RNAi concentration of 10 nM. The cells were incubated at 37 ° C in 5% CO<sub>2</sub>. The first media was changed after 12 hours and subsequently replaced every 72 hours. Appropriate negative controls are used during each time point. Negative controls are gene sequences used during transfection studies to look for any non-specific effects on gene expression. They are siRNA sequences that do not target any gene product and are essential for determining siRNA delivery efficiency. When cells are transfected with these sequences there should not be any effects on gene expression ([www.ambion.com](http://www.ambion.com)).

### **5.2.3 Osteogenic Induction**

Following the transfection of the ADSCs with the Lipofectamine – RNAiMAX duplex, the cells were induced with standard osteogenic media at two different concentrations: 1X (optimal induction concentration) and 0.1X (sub-optimal induction concentration). As control, uninduced cells treated without any osteogenic induction supplements (i.e. 0X category) were maintained.



#### 5.2.4 RNA isolation and Real-time PCR analysis of ADSCs

The RNA isolation and real-time PCR analysis was done as mentioned in the previous chapter. Following reverse transcription and cDNA synthesis, real-time PCR was done to detect ATF5, Osteocalcin,  $\beta$ -actin and ATF4 genes. Standards for the ATF4 and ATF5 genes were prepared as per the techniques outlined in the previous chapter. The primer sequences used were:

| Gene           | Primer Sequence  |
|----------------|--|
| ATF 4          | 5'-TGACCACGTTGGATGACACT-3'<br>5'-CCTGGTCGGGTTTTGTAAA-3'    |
| ATF 5          | 5'-GTATTGACCTCCTGGCCTCA-3'<br>5'-CCTTCATTCCAACCCCTCT-3'    |
| Osteocalcin    | 5'-TGTGGCATCCACGAAACTAC-3'<br>5'-GGAGCAATGATCTTGATCTTCA-3' |
| $\beta$ -Actin | 5'-TGTGGCATCCACGAAACTAC-3'<br>5'-GGAGCAATGATCTTGATCTTCA-3' |

**Table 5.1** – Primer sequence of genes used for real time PCR in gene silencing experiment

## 5.3 RESULTS

### 5.3.1 Expression of ATF4 during osteogenic differentiation in ADSCs

Real time PCR analysis of ADSCs for ATF4 gene expression revealed that the pattern was variable from donor to donor. In three out of the ten samples analyzed, the expression pattern was similar to that seen in human fetal osteoblasts (hFOBs). The similarities in pattern of these samples to the expression in hFOBs suggest that these donor samples might be an ideal source for ‘osteogenically inclined’ ADSCs (Fig 5.1).

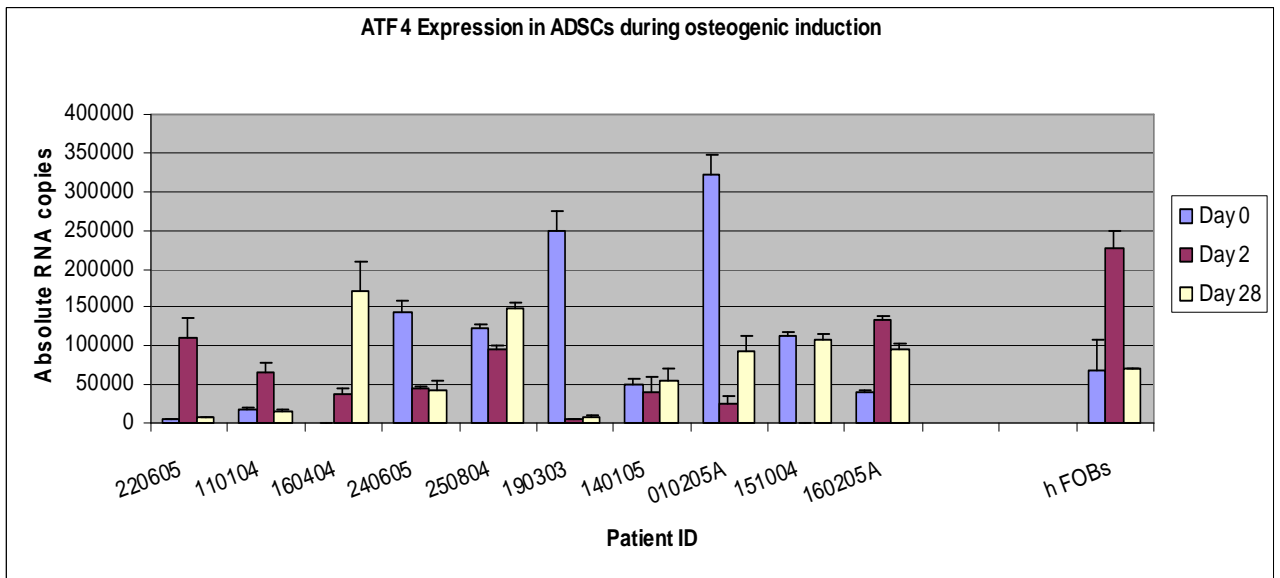


**Fig 5.1 – ATF4 expression pattern in ADSCs.** In three of the ten samples tested, the ATF4 expression increased during the second day and dropped drastically by the twenty-eight day. This pattern was similar to that seen with hFOBs cell lines. The lack of a consistent response in all the ADSC samples may be due to the differences in the ‘intrinsic osteogenic potential’ among the cells.

### **5.3.2 Silencing of ATF5 expression by Stealth™ RNAiMAX in ADSCs**

The real time PCR analysis of the ADSCs showed that in all the four patient samples, the ATF5 expression was lower in the groups that had been transfected with the RNAi duplex complexes (Figs 5.2), indicating that the transfection was effective in silencing the ATF5 gene expression. However a significant drop in the expression was not seen across all the samples. The expression of ATF5 in the non-silenced samples also followed such a trend. Fig 5.2A shows a sample in which significant drop in ATF5 expression after silencing was seen only in day 1 at one time point (indicated with the arrowhead) and in day 5 at two time points. On the contrary, Fig 5.2 B shows a sample in which significant drop in ATF5 expression was seen across all the time points.

In order to negate any discrepancy from cell numbers, in all the donor samples the ATF5 copy numbers were normalized against  $\beta$ -actin copy numbers for the specific time points.

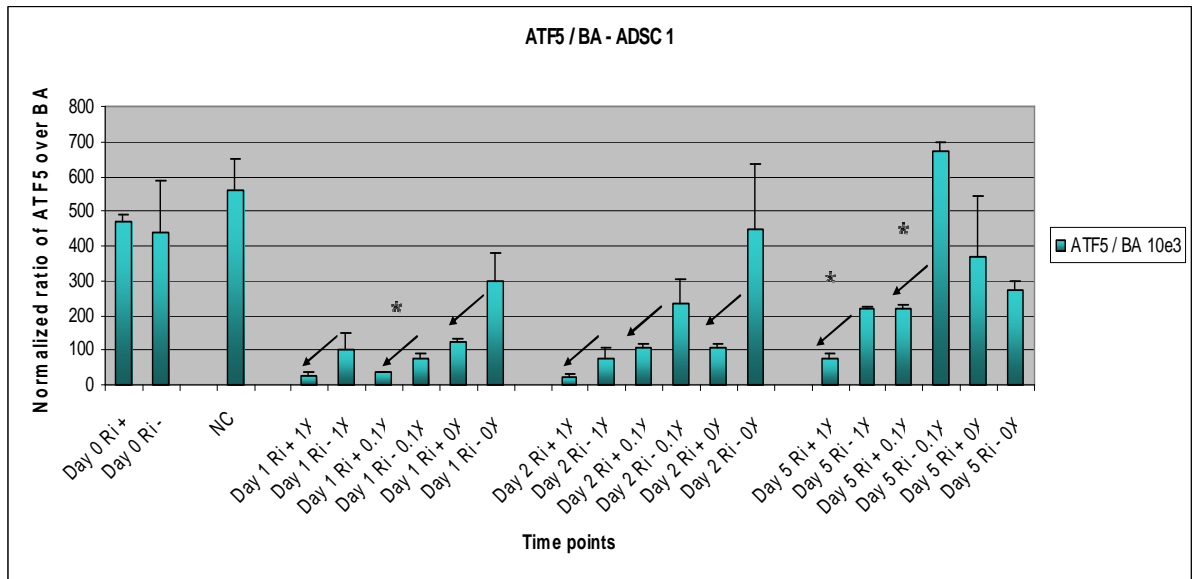


**Fig 5.2 A**

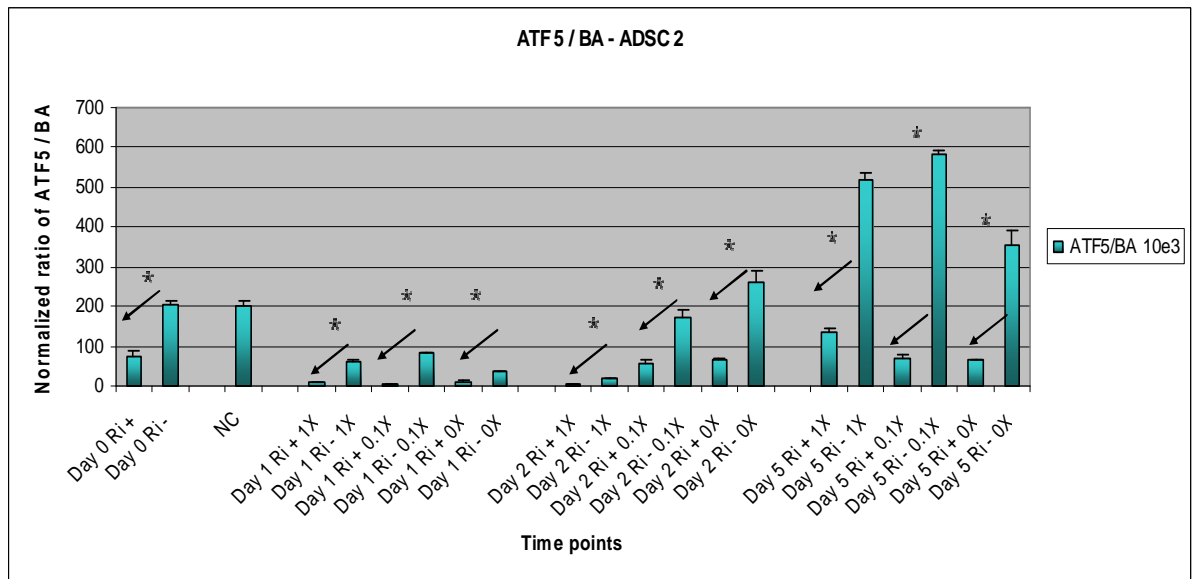


**Fig 5.2 B**

**Fig 5.2 - ATF5 expression normalized to  $\beta$ -actin.** In all the donor samples tested there was a decreased expression of ATF5 in the gene silenced groups (*Ri* + ). The time point at which silencing was maximum varied from sample to sample, with some having a pronounced response at day 1, while others having at day 2. (A representative graph of two donor samples are being shown in Fig 5.2 A and B).

### **5.3.3 Osteocalcin expression in the ADSCs**

Osteocalcin expression in the ADSCs that have been silenced with ATF5 RNAi showed a variable expression (Figs 5.3). However, in all of them there was a consistently significant difference in the expression levels of the Day 2 samples. The day 2 uninduced and gene silenced groups (*Day 2 Ri+ subgroups*) showed a significantly higher expression than the corresponding uninduced and non-silenced groups (*Day 2 Ri- subgroups*). Among the same set of samples, the osteocalcin levels were also found to be significantly higher in the gene silenced that were either sub optimally induced (0.1X) and uninduced (0X) groups, compared to the induced samples that were gene silenced.

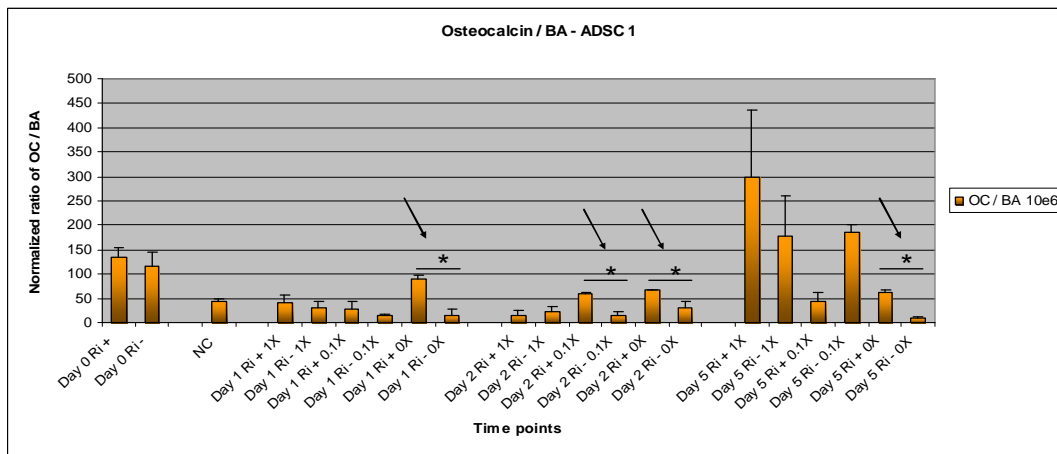


**Fig 5.3 A**

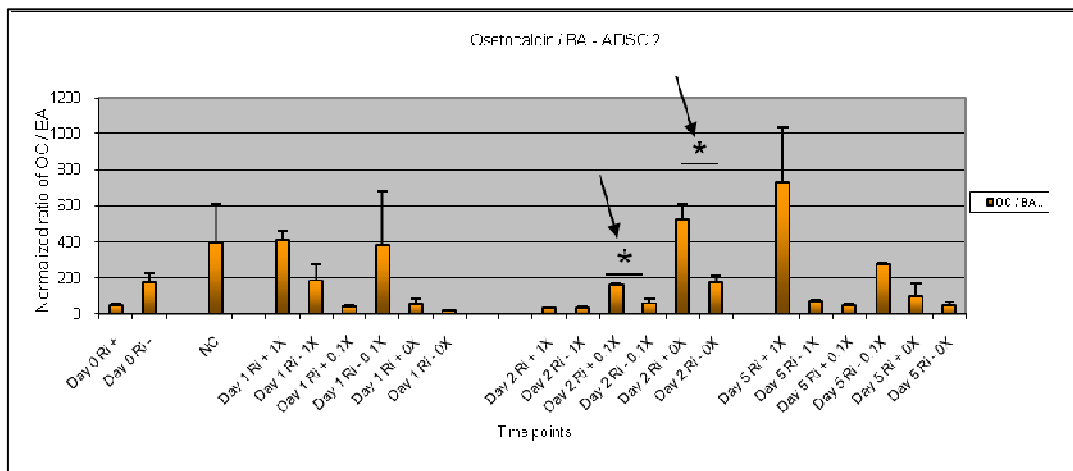


**Fig 5.3 B**

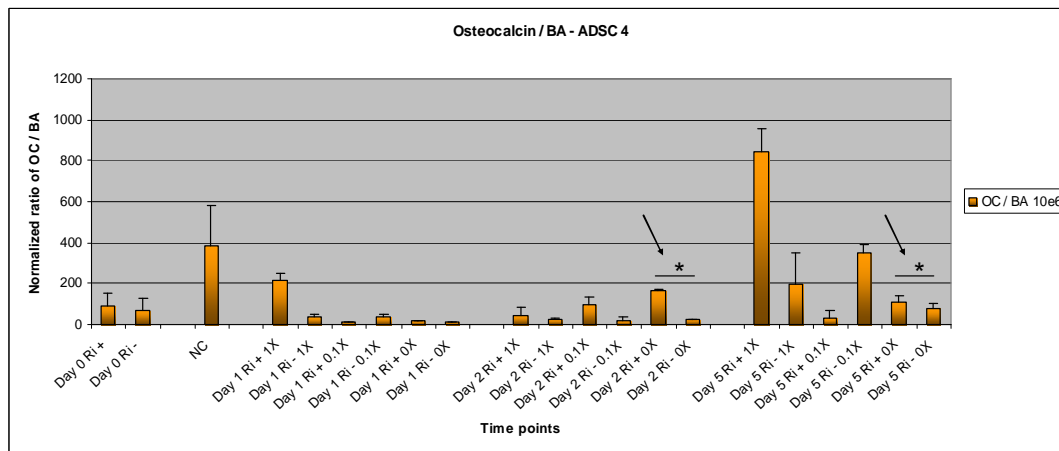


**Fig 5.3 C**

**Fig 5.3 -** Osteocalcin expression normalized to  $\beta$ -actin. There were significant increases in the expression levels of osteocalcin in the gene silenced groups at varying time points (Ri + subgroups). All the samples showed increased expressions, at different time points, in the sub optimally induced (0.1X Ri +) and uninduced (OX Ri +) groups which were gene silenced. The arrow heads show the relevant time points at which significant differences were seen.

#### **5.3.4 ATF4 expression in the ADSCs**

The ATF4 expression did not show the consistent changes seen with osteocalcin, indicating that the expression patterns of ATF4 was highly variable. In a few of the samples, a significantly increased expression of ATF4 was seen in the ATF5 gene-silenced groups at day 2 (Fig 5.4B). However, in three of the four samples, the optimally induced and ATF5 silenced groups (1X) showed a significant increase in ATF4 compared to the corresponding non-silenced groups.

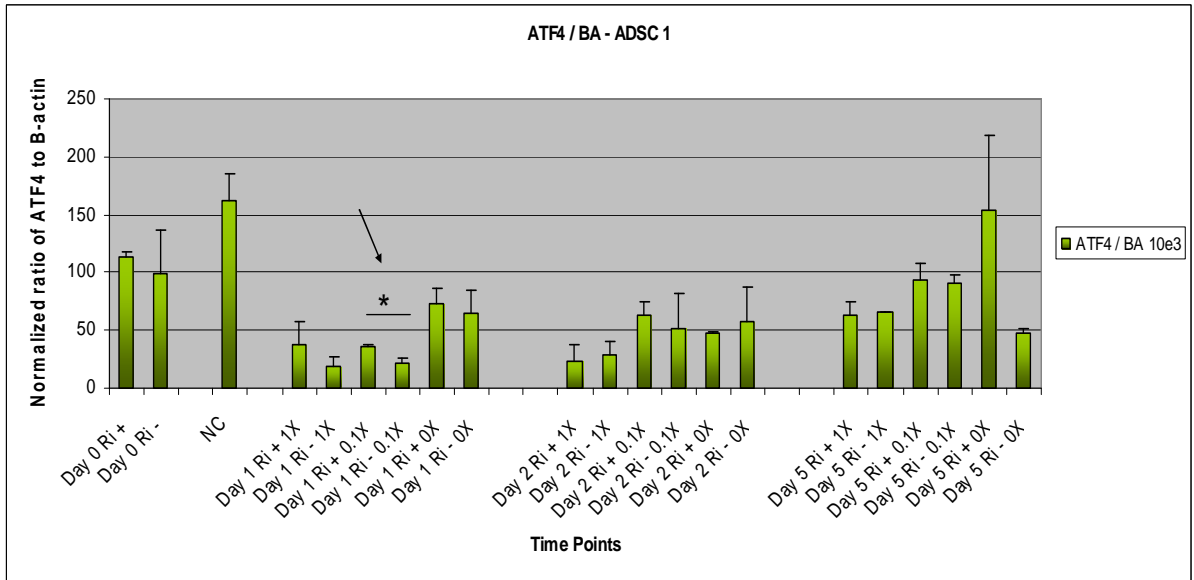


**Fig 5.4 A**

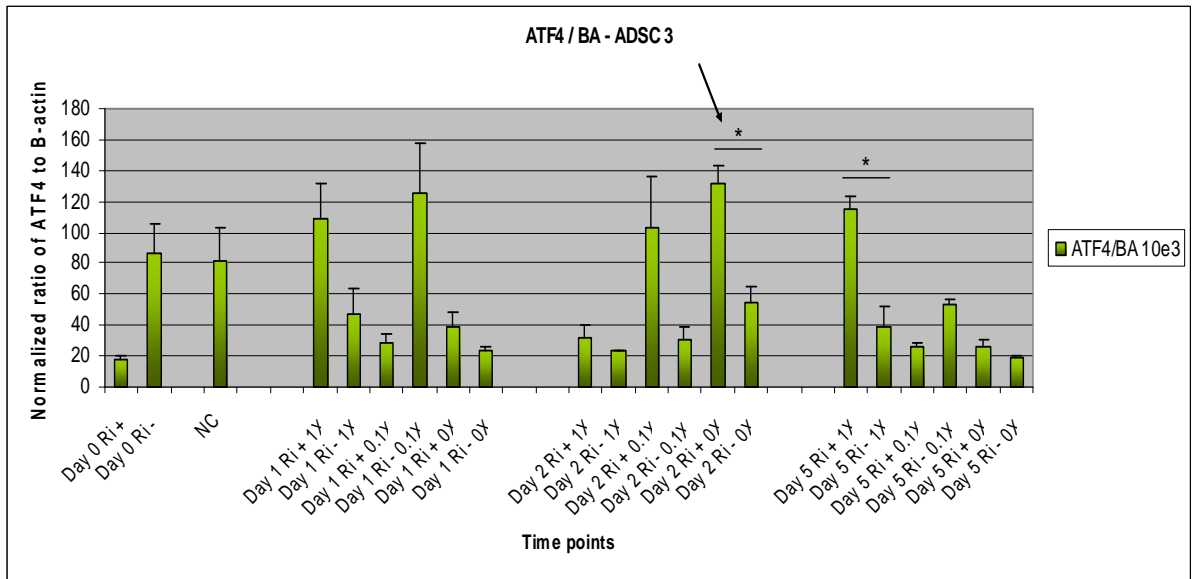


**Fig 5.4 B**

**Fig 5.4 - ATF4 expression normalized to  $\beta$ -actin.** Some of the ADSC samples showed an increased expression of ATF4 in the ATF5 silenced groups (arrow headed groups in Figs 5.4 A and B). However the significance was not observed across all the donor samples (data not shown).



## 5.4 DISCUSSION

ADSCs are being extensively studied for the purpose of cell replacement therapy. One such area wherein there is much scope and potential for cell regeneration therapies is bone tissue engineering. ADSCs have been shown to be able to differentiate towards cells of the osteogenic lineage when exposed to right set of stimuli (Zuk et al., 2000). However, the basic biology that governs the ability of these non-bone origin mesenchymal cells to form bone tissue has yet to be clearly outlined. One of the genes that is shown to have the potential to modulate this behavior in non-bone cells, as mentioned earlier, is ATF4.

To this end, we decided to look for the expression pattern of ATF4 gene in ADSC, both before and during induction for a period of 28 days. From our results, we were able to see that three out of ten patient samples analyzed for this gene, showed a pattern similar to that seen in human osteoblast cell lines (Fig 3.1). The gene levels increased significantly by the second day of induction and fell drastically by day twenty eight. As mentioned earlier ATF4 has been shown to interact with Runx2 in activating osteocalcin expression (Xiao G et al., 2005). Since Runx2 is one of the earliest markers to be elevated during the process of osteogenesis, the expression pattern where ATF4 peaks early and falls down later on would fall in line with the argument that ADSCs undergoing osteogenic differentiation may be influenced by ATF4 in adopting the osteogenic lineage. However, this gene may not alone be enough in influencing osteogenesis in ADSCs, as seen by the lack of a consistent expression pattern seen in many of the ADSCs.

The RNA interference mediated silencing of ADSCs showed that there was a significant drop in expression of ATF5 gene in the ADSCs (Fig 3.2 A and B). The fall in expression was more pronounced at day 2 and day 5 time points of the study. The absence of a significant drop in expression among the Negative control groups (NC) for each of the ADSCs in Figs 3.2 indicates that the silencing was effective.

The osteocalcin expression in these ATF5 silenced ADSCs followed an interesting pattern. As could be seen from Figs 3.3, in all the ADSC samples, there was a significantly elevated expression of osteocalcin in the silenced groups (*Ri+ group*) at day two and five compared to the unsilenced group (*Ri – group*). The conventional protocols for osteogenic induction advice an optimum induction factor concentration of 1X to achieve the most efficient osteogenic outcome. In our study, in a few of the ADSC samples (Figs 3.3) the osteocalcin was expressed significantly at even the suboptimal inducing concentration of 0.1X. In all the ADSC samples, at all time points, there was a significant expression of osteocalcin even in the absence of inducing factors (0X subgroups in Figs 3.3). While in a few of the ADSC samples this pattern was more pronounced at day 5 (*Day 5 Ri + 0X* subgroups in Fig 3.3), in a few of the same and the remaining it was more pronounced at day 2 (*Day 2 Ri + 0X* subgroups in Figs 3.3).

The ATF4 expression on the other hand, was not very consistent in the tested ADSC samples. The normalized ratio of ATF4 to  $\beta$ -actin showed that there was increased expression of ATF4 in the ATF5 silenced and suboptimally induced / uninduced groups (*Ri +and 0.1X / 1X*) at varying time points (Figs 3.4). In some of the samples this

difference were more pronounced in the *Ri + 0.1X / 1X subgroups* at day 1, while in others it was seen in the same subgroups at either day 2 or 5.

However a significant over expression of ATF4 in the ATF5 silenced subgroups was seen only with ADSC 3 (Fig 3.4 B) where ATF4 was higher in the day 2 ATF5 silenced and uninduced group (*Day 2 Ri + 0X*).

Osteocalcin has traditionally been considered as one of the most specific markers for osteogenic differentiation (Ducy P et al., 2000). These expression patterns of osteocalcin seen in our study, especially the groups in which there were no induction factors present (0X subgroups) indicate that silencing the expression of ATF5 maybe sufficient in some cases to trigger osteocalcin expression. A possible explanation for this observed phenomenon could be that repression of ATF5 triggers some alternate pathway or activates transcription factors that could act to increase osteocalcin expression. At this point, however the same could not be said about ATF4. Though one would have expected a consistent over expression of ATF4 in an ATF5 silenced situation, the lack of a consistent and significant pattern in this study might mean that ATF4 and ATF5 might not have mutually reciprocal roles in modulating osteogenesis in ADSCs. On the contrary, ATF4 – ATF5 interaction might not have been consistently picked up due to the genetic variability in the samples being analyzed. The donor variability that account for varying patterns of gene expression as explained in Chapter 4 could be operational here as well. The preliminary ATF4 expression done on the same set of samples done for the gene chip analysis during the PhD work of Leong TWD also showed this variability in ATF4 expression (Fig 3.1). This may be attributed to the possibility that ADSCs from

different human beings differ in their 'intrinsic osteogenic potential' i.e. some of the ADSCs are better at responding to osteogenic stimuli in the environment and hence undergoing osteogenic differentiation, while others may not be that good at the same. Such a variability occurring here could not also be completely ruled out.

## **5.5 CONCLUSION**

From this study using RNAi against ATF5, it was shown that ATF5 gene could be effectively silenced in ADSCs. The expression pattern of osteocalcin among the silenced ADSCs demonstrated that in most of the samples tested, ATF5 silencing was enough to cause a significant over expression of osteocalcin. However, the same could not be said about ATF4. While there was an increased expression of ATF4 in most of the ATF5 silenced groups which were either sub optimally induced (0.1X) or uninduced (0X), a statistically significant result was seen in only one of the four ADSC samples tested. However this phenomenon could be due to the differences in the 'intrinsic osteogenic capability' of the ADSCs tested. Therefore, it may be possible that ATF4 and ATF5 might interact by themselves or through some other mediators, in inducing osteogenesis in ADSCs.

## **CHAPTER 6**

### **CO-TRANSFECTION AND EXPRESSION OF ATF4 AND ATF5 IN HEK CELLS**

#### **6.1 INTRODUCTION**

One of the genes that have been implicated in inducing osteogenic differentiation in non-osteoblast cells is ATF4 (Activating Transcription Factor 4). Though the gene for this protein is ubiquitously expressed in a wide variety of tissues like brain, thymus, liver and the lung, the protein is only expressed in mature osteoblasts (Yang X et al., 2004). When NIH3T3 fibroblasts, which in the native state do not express ATF4 protein were transfected with siRNA to a ubiquitin ligase that normally cleaves the ATF4 protein in non-osteoblast cells, they began to express ATF4 and osteocalcin. These were conclusive evidences for the role of ATF4 in mediating osteogenic differentiation in non-osteoblast cells. Members of the ATF family have been well known to interact with each other forming homodimers and heterodimers. Some of these interactions are the key processes that mediate important cellular functions (Ameri K et al., 2007). The interaction of ATF4 with Runx2 has been shown to increase the expression of osteocalcin gene in non-osteoblast cell lines (Xiao G et al., 2005). Deletion analysis studies have shown that this interaction occurs primarily through the leucine zipper region of ATF4.

Thus it could be inferred that interactions between key transcription factors like ATF4, Runx2 etc. play a significant role in deciding the fate and phenotype of immature cells.

From the previous chapter it was shown that silencing the expression of ATF5 mRNA causes a significant increase in the expression of osteocalcin. While in some of the ADSC

sample studied this occurs at suboptimal induction doses (0.1X subgroup), in a few of them a significant expression is seen even in the absence of any induction factors (0X subgroup). The rise in osteocalcin levels in the absence of induction factors imply that silencing of ATF5 in some way triggers some repressed pathways that would not have otherwise lead to osteocalcin expression. Similarly, it was also seen that in some of the ADSC samples, there was an increased mRNA expression of ATF4 when ATF5 gene had been silenced, though a significant difference in expression was seen in only one of the four ADSC samples tested. This lack of a significant expression of ATF4 in the other three samples might be because of their differences in their intrinsic potential of undergoing osteogenic differentiation.

Based on the well known fact that members of the ATF family have the potential to interact among themselves as well as with transcription factors of other groups and the inverse gene expression profile of ATF4 and ATF5 that was saw in the gene silencing experiments, it was decided to explore the possibility that ATF4 and ATF5 may also have the potential to interact with each. In such an eventuality, the interaction between ATF4 and ATF5 may in some influence the osteogenic differentiation potential of ADSCs.

In order to look for the possibility of a binding potential between ATF4 and ATF5, Human Embryonic Kidney (HEK) cell lines were cotransfected with plasmids cloned with ATF4 and ATF5 genes. Subsequent to the co-transfection, the cells were lysed and the total protein isolated. Following this, co-immunoprecipitation was done on the cell lysates. In this procedure, the antibody against one of the proteins (e.g. anti ATF5) was used to pull down the proteins from the lysate and subsequently immunoblotted with the

antibody against the second (e.g. anti ATF4). If ATF4 and ATF5 are indeed capable of binding with each other, such a pull down with using one antibody, should bring along with it its binding partner, which could then be detected by the second antibody.

### 6.1.1 Characteristics of the Vector used for generating plasmid

The vector used for the initial cloning of the inserts and the subsequent transfection of the HEK cell lines was the pCDNA6/His<sup>TM</sup> A vector (Invitrogen). This is a 5.2 kb vector that has been widely used for the transient and stable over expression of proteins in mammalian systems. Like most mammalian vectors, this vector possesses a Human Cytomegalovirus immediate-early (CMV) promoter, designed for high level protein expression in mammalian cell lines. Apart from the CMV promoter, the vector possesses an Ampicillin resistance gene for selecting clones in bacteria, Blastidicin resistance gene for selection of stable cell lines and a Multiple cloning site with a 6X Histidine Tag preceding it (*pcDNA manual, Invitrogen., 051302*).

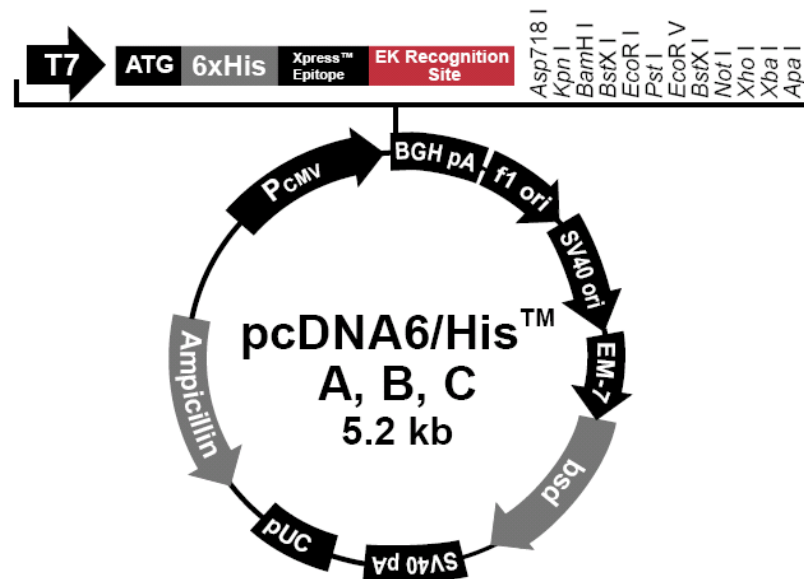


**Fig 6.1** - Vector map of pcDNA6/His<sup>TM</sup> A ([www.invitrogen.com](http://www.invitrogen.com))

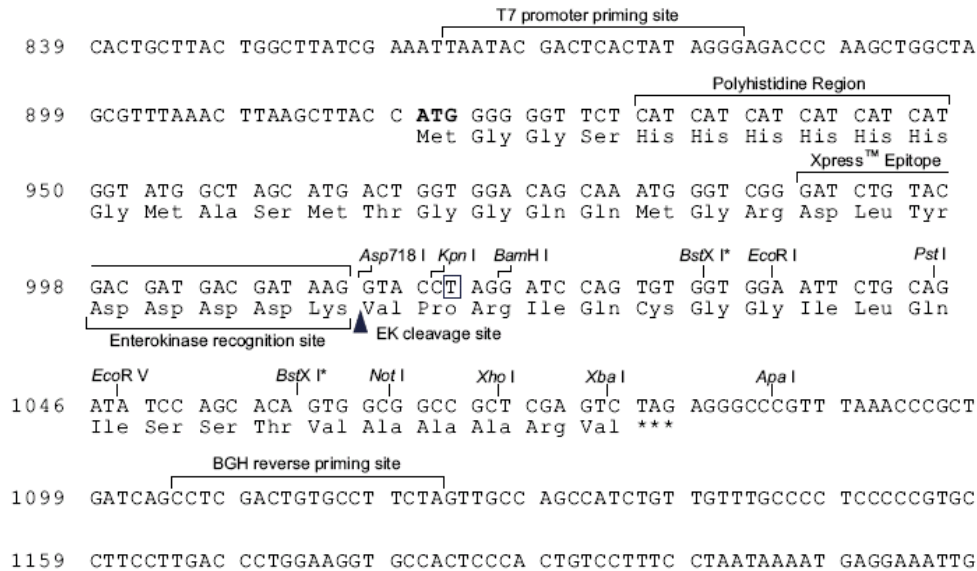


**Fig 6.2** – Multiple Cloning Site (MCS) of pcDNA6/His™ A ([www.invitrogen.com](http://www.invitrogen.com))

## 6.2 MATERIALS AND METHODS

### 6.2.1 Vector cloning and preparation

The initial cloning of pcDNA6/His™ A vector was done in Novablue™ ( Novagen ) DH 3α cells. Briefly, the transformation was done by adding about 10 ng of the vector to 20 µl of Novablue™ cells in a microfuge tube and placing on ice for 5 minutes. At the end of 5 minutes, the tube was subjected to heat shock by placing in a water bath preheated to a temperature of 42° C for exactly 30 seconds and then again placed on ice for 2 minutes. At the end of the time the Novablue™ cells were plated onto an agar plate, containing ampicillin at a working concentration of 50 µg/ml and kept for transformation overnight at a temperature of 37° C. The following day , a few colonies were picked and grown in 5 ml of LB medium (Luria Bertani) for 12 to 16 hours in a rotating shaker at a speed of 240 rpm and temperature of 37° C . The tubes containing the culture media were then spun down and the plasmids extracted using a GeneJet™ Plasmid Miniprep Kit (Fermentas).



### 6.2.2 Insert design and preparation

Two different inserts were designed and prepared for the purpose of cloning and expression.

1. **ATF 5 full length** – Having the entire 849 base pair corresponding to the coding sequence of the gene.
2. **ATF 4 full length** – Having the entire 1056 base pair corresponding to the coding sequence of the gene.

For the process of cloning the inserts into the vectors, **EcoR1** and **Xho1** (Fermentas) were the restriction enzymes chosen. The choices of these two enzymes were based on the following reasons:

1. By choosing two different enzymes for digestion and thus performing a double digestion, it would be possible to generate two different sticky ends, and thus perform a Directional cloning, thereby ensuring that the insert and vectors would ligate only in the proper orientation.
2. The two enzymes are compatible for double digestion with a common buffer – Buffer B (Fermentas).

The inserts were generated from Human MGC (Mammalian Gene Collection) cDNA clones for ATF4 and ATF5 (Open Biosystems Inc.) by Polymerase Chain Reaction (PCR).

The primers for generating the inserts from the mammalian cDNA were designed incorporating the restriction sites for **EcoR1** and **Xho1** into them, so that the PCR

products would have these sites. A subsequent digestion of the inserts with these enzymes would yield products with sticky ends that would bind to the appropriate sites in the vector digested with the same enzymes. The primer sequences for the different inserts were:

| Insert            | Primer Sequence  |
|-------------------|--|
| ATF 5 Full length | EcoR1 GCTAAGAATTCATGTCACCTCCTGGCGA<br>Xho1 AATAACTCGAGCTAGCAGCTACGGGT          |
| ATF 4 Full length | EcoR1 ATGCGGAATTCATGACCGAAATGAGCTTCCTG<br>Xho1 AATAACTCGAGCTAGGGGACCCTTTTCTTCC |

**Table 6.1** – Sequences used for generation of inserts

In order to decrease the incidence of mutations in the cloned inserts, PCR reactions were done using high fidelity *Pfu Polymerase* enzyme (Fermentas). The thermocycling conditions were:

Initial denaturation at 94° C for 5 minutes followed by 35 cycles of denaturation at 94° C for 1 minute, annealing at 55° C for 1 minute, extension at 72° C for 2 minutes and a final extension at 72° C for 6 minutes. The PCR products were then verified for the size of the products by running on a 1% Agarose gel and comparing with GeneRuler™ ladder (Fermentas).

### **6.2.3 Restriction enzyme digestion of the vector and inserts**

Both the vector and the inserts were digested using EcoR1 and Xho1 restriction enzymes. As mentioned earlier, since the inserts had the restriction sites for each of these enzymes incorporated into them during the subcloning process, digestion would yield products that would fit into the vector in the proper alignment. To carry out the enzyme digestion, the following components were assembled in a PCR tube: 5 µg of the vector or insert, 20 µl of 10X Buffer Tango™ (Fermentas), 10 µl of EcoR1, 10 µl of Xho1 and finally deionized water was added to reach a final reaction volume of 100 µl. The reaction mixture was then incubated at 37° C for 16 hours in a thermocycler. At the end of 16 hours the enzymes were inactivated by heating at 80° C for 20 minutes. As control, reaction mixture having only the vector or inserts without adding any of the restriction enzymes were used. Since the chances of re-ligation of the vector were minimized by using two different restriction enzymes, Calf Intestinal Alkaline Phosphatase was not used following digestion.

Following digestion of the vector, the cut vector was run against the uncut vector on a 1% agarose gel. Since the cut vector becomes linear, it migrates at a different rate when compared with the uncut vector. This distinguishes between the two different sets of vectors. Once the band of interest (the completely cut vector) was identified in the gel, it is cut with a clean razor blade and transferred to a microfuge tube. The digested vector was then isolated from the agarose gel by using Gel purification kit ( vCellScience ) and stored at – 20° C , till further use.

The digested inserts were not gel purified; rather they were purified using Qiagen PCR purification kits. The purified inserts were then run on 1% agarose gel, to ascertain the quality of the purified products.

## **6.2.4 Cloning of the inserts into the vector**

### **6.2.4.a Ligation**

Following purification of the digested vector and inserts, the quantity of each were measured for the next step of ligation. The two components were ligated in a molar ratio of **1:4** of vector: insert DNA. The calculation was obtained based on the following formula:

$$\text{ng of vector} \times \frac{\text{kb size of insert}}{\text{kb size of the vector}} \times \text{molar ratio of } \frac{\text{insert}}{\text{vector}} = \text{ng of the insert}$$

Based on the above formula for a ligation reaction using 100 ng of the vector, the required molar concentration of the insert comes to around 50 ng .

The final ligation mixture consisted of 100 ng of the vector DNA, 50 ng of the insert DNA, 2 µl of 10 X T4 DNA Ligase buffer, 1 µl of T4 DNA Ligase ( Fermentas) and water, added to reach a final reaction volume of 20 µl. The reaction mixture was incubated at 25° C for 4 hours. At the end of the reaction, no heat inactivation was performed. Roughly 2 µl of the ligation mixture was used for transforming about 20 µl of competent NovaBlue™ E.Coli cells.

#### **6.2.4.b Transformation**

The transformation was done in competent NovaBlue™ E. coli cells. These are a commercial variety of DH3  $\alpha$  cells. These cells are the usual hosts of choice for the primary cloning of the target plasmid, as they have high transformation efficiency and yield large quantities of high quality DNA. These cells lack the gene coding for the T 7 RNA polymerase and hence cannot be used under expression conditions.

For the purpose of transformation, about 20  $\mu$ l of frozen competent cells in a microfuge tube were allowed to thaw on ice for about 2 – 5 minutes. Following this, about 2  $\mu$ l of the ligation mixture (containing less than 10 ng of DNA) was added to the cells and gently stirred. The mixture was immediately placed on ice and incubated for 5 minutes. Subsequently the tubes were placed for exactly 30 seconds in a water bath at 42° C and then placed back in ice for 2 minutes. This heat shock protocol would ensure that the bacterial walls become permeabilized for the uptake of the added DNA. At the end of this procedure the transformation mixture was plated into a pool of about 40  $\mu$ l SOC medium and then spread evenly on the surface of an agar plate containing ampicillin at a working concentration of 50  $\mu$ g/ml. The plates were incubated overnight at 37° C and subsequently checked for the presence of positive colonies. As a control, plating was done using untransformed competent cells, which technically should not form colonies as they do not possess the ampicillin resistance gene contained in the pCDNA6/His™ A recombinants.



ladder. As a control, the colony PCR reaction was done on the uncut pCDNA6/His<sup>TM</sup>A plasmid. The size of the prominent band would correspond to the total region between the primers.

Once the correct identities of the colonies were established by colony PCR, those colonies that contained the insert were then grown in a 5 ml tube containing LB medium by incubating at 37° C for 12 to 16 hours in a shaker at a speed of 240 rpm. The plasmids were then extracted and purified from the 5 ml broth using a GeneJet<sup>TM</sup> Plasmid Miniprep kit. The plasmids were then sequenced in an ABI sequencing machine with pGEM vector as the control. The results were analyzed on Chromas Lite<sup>TM</sup> software. The alignment of reading frames and absence of mutations was confirmed.

### **6.2.5 Estimating the molecular weight of the proteins to be expressed**

The molecular weights of the proteins being expressed were based on the sum of the total number of bases of the cloned insert plus the additional bases between the start codon of the vector and the point of insertion of the insert within the MCS. Based on the vector map (Fig 4.2), the number of additional bases between the start codon (ATG) and the EcoR1 site is exactly 115 bp. The total base pair lengths of ATF4 and ATF5 are 1056 and 849 bp respectively. Adding the extra bases, ATF4 mRNA would have a total length of 1171 bp, equivalent to 390 amino acid sequences and ATF5 mRNA would have total length of 964 bp, being equivalent to 321 amino acid sequences. From the assumption that the average molecular weight of a single amino acid is 0.1 kD, the expected

molecular weight of our expressed products would be **39 kD** for ATF4 and **32 kD** for ATF5.

#### **6.2.6 Co-Transfection of ATF4 and ATF5 plasmids into HEK293 cells**

The colonies that generated plasmids having the right sequence of the cloned genes were then grown in large numbers for plasmid isolation. Parallel to this, HEK 293 cells were grown in and maintained in DMEM supplemented with 10% Fetal Bovine Serum (Gibco). The protocol used for transfection was optimized based on the guidelines given by the company (Invitrogen).

A few days before the transfection procedure, the HEK cells in culture were trypsinized and counted. They were subsequently plated as a lower density in 100 mm culture dishes (TPP plastics), so that on the day of the transfection, they would be 60% to 80% confluent. The cells were maintained in DMEM supplemented with 10% FBS, without the use of any antibiotics. On the day of the transfection about 2 µg each of ATF4 and ATF5 plasmids were diluted in 750 µl of DMEM, without any supplemented FBS in a 50 ml Falcon tube. To this mixture about 20 µl of Plus reagent™ (Invitrogen) was added and incubated at room temperature for 20 minutes. Plus reagent™ is a proprietary transfection enhancing agent, which is supposed to increase the transfection efficiency. In a separate Falcon tube, 30 µl of Lipofectamine™ Reagent (Invitrogen Catalog : 18324-012) was diluted in 750 µl of DMEM without serum. At the end of 20 minutes of incubation, the plasmid-Plus reagent™ complex was mixed with the Lipofectamine™ reagent and further incubated for 20 minutes. While the complexes were being formed, the media on



the plates were replaced with 5000  $\mu$ l of DMEM supplemented with 10% FBS. At the end of the incubation period, the complexes were added onto the 100 mm culture dishes to reach a final volume of 6500  $\mu$ l. The culture dishes were maintained in an incubator at 37° C in 5% CO<sub>2</sub> for 5 hours, at the end of which the media in each plate were topped up to 10 ml. The transfected cells were maintained in the incubator for 48 hours, to achieve the optimal protein expression. As control, untransfected HEK cells were grown and maintained in similar conditions for the required time frame.

### **6.2.7 Immunoprecipitation of ATF4 and ATF5 from HEK cell lysates**

After 48 hours, the cells were lysed in 1% Nonidet P-40 Lysis buffer. The buffer is composed of 50 mM Tris-HCl (pH 7.4), 1% Nonidet P-40, 150 mM NaCl, 1 mM EDTA, 1 mM NaF, 1 mM Phenylmethylsulfonyl fluoride, 1 mM Na<sub>3</sub>VO<sub>4</sub> and 100X Protease Inhibitor. The cells were lysed at 4° C for 20 minutes and the lysate collected.

For immunoprecipitation, the supernatants were mixed with 40  $\mu$ l of Immobilized Protein G Plus beads (Catalog No: 22851, Pierce) at room temperature for 1 hour and then centrifuged at 14,000 rpm for 2 minutes. The precipitated beads were discarded and the total protein concentration estimated in the cell lysates. For each immunoprecipitation about 1000  $\mu$ g of the total protein was incubated with 3  $\mu$ g of the respective antibody overnight at 4° C on a rocker. The following day, the immunoprecipitates were collected by adding 40  $\mu$ l of the Immobilized Protein G Plus beads and incubation for 1 hour at room temperature. The immunoprecipitate-Protein G bead complex was collected by centrifuging at 14,000 rpm for 2 minutes. The precipitates were subsequently washed five times in cold PBS. The beads with the protein complexes were treated with 20  $\mu$ l of SDS

buffer (with added  $\beta$ -mercaptoethanol) and denatured by heating at 90° C for 10 minutes. The proteins were then resolved by SDS-Page and transferred to nitrocellulose membrane. Western blot was done with the corresponding antibodies.

Primary antibodies used for the detection of the respective proteins were:

|   |   |        |
|---|---|--------|
| Rabbit anti human ATF4 (Abcam, ab23760) | - | 1:1000 |
| Goat anti human ATF5 (Abcam, ab1370)    | - | 1:2000 |

For ATF4 detection, the secondary antibody used was anti-Rabbit antibody conjugated to HRP (Horse radish peroxidase) enzyme, raised in goat (Zymed, 62-6120), used at a concentration of 1:15,000. For ATF5 detection, the secondary antibody used was anti-Goat antibody conjugated to HRP, raised in rabbit (Abcam, ab6741), used at a dilution of 1:6000.

## 6.3 RESULTS

### 6.3.1 Insert preparation

The inserts after PCR were run on a 2% gel and the product lengths verified. From Fig 6.3 A and B, it can be seen that the size of the inserts corresponded to those predicted from the initial calculation. ATF4 inserts corresponded to a product size of around 1050 bp (1056 bp – actual length) and the ATF5 inserts corresponded to a size of around 900 bp (849 bp – actual length)

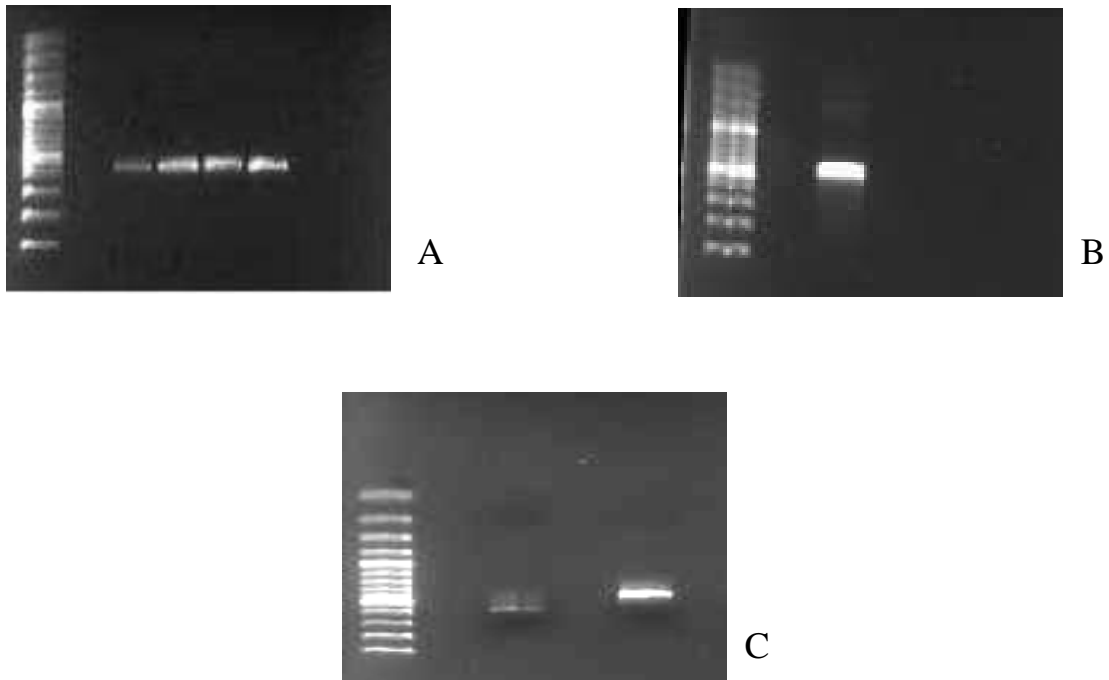


**Fig 6.3 – Gel picture of the inserts obtained from PCR.** ATF4 (Fig 6.3 A) corresponds to the 1050 bp marker, while ATF5 corresponds to 900 bp marker (Fig 6.3 B). Running the two inserts on the same gel gave a clearer distinction between the two (Fig 6.3 C). The one on the left is the ATF4 insert and the one on the right is the ATF5 insert.

### 6.3.2 RE cut and uncut vector

The vector after double digestion was run on a gel. The cut vector, being linear, ran at a slower pace (Fig 6.4, red boundary) when compared to the uncut vector (Fig 6.4, turquoise boundary), which was supercoiled. This was the basis of delineating separating the cut vector from the native uncut vector.

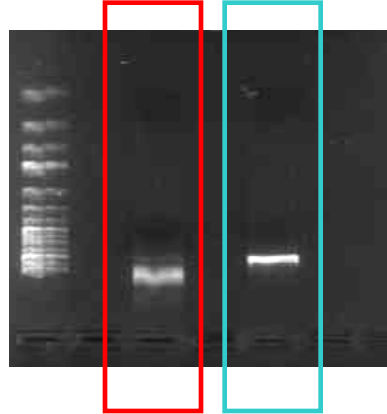


**Fig 6.4 – Gel picture of the vector after Restriction Enzyme digestion.** The uncut vector (turquoise box) having a weight of 5200 bp, being supercoiled appears to run faster than the cut vector (red box). This is because the linear structure of the cut vector impedes its paces through the gel, causing it to appear lagging behind the uncut vector.

### 6.3.3 Colony confirmation through Colony PCR

Colony PCR was done on the transformed colonies to identify those colonies which had taken up the correct set of inserts. The estimated product length for the ATF4 inserts within the plasmid was around 1100 bp (Fig 6.5 A) and the same for the ATF5 inserts were close to 950 bp (Fig 6.5 B). The extra base lengths detected in each of the inserts (when compared to the native PCR product above) are the extra bases flanking the insets in the MCS region of the vector and being amplified by the colony PCR primers.

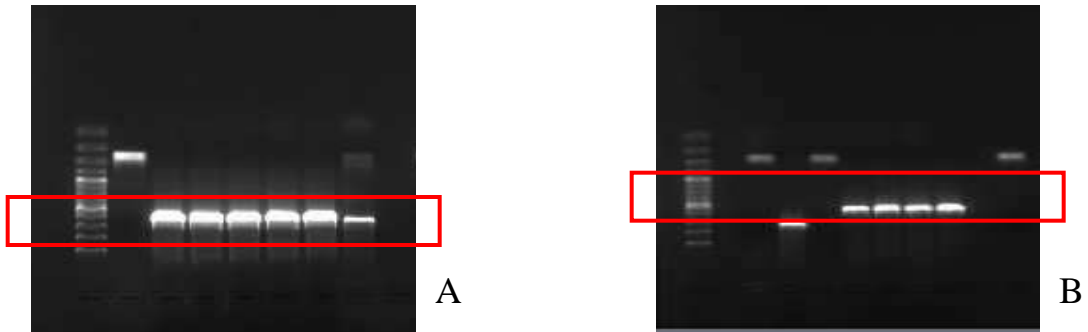


**Fig 6.5 – Gel picture of the inserts obtained from colony PCR.** ATF4 insert (Fig 6.5 A) within the plasmid corresponds to the 1100 bp marker, while ATF5 corresponds to 950 bp marker (Fig 6.5 B)

### 6.3.4 Western Blot with Anti-His antibody

Cell lysates were immunoblotted with anti-His antibody. Three distinct bands were observed when the blots were stained (Fig 6.6A). The top most band was seen at a molecular weight of around 80 kD, the second one was at around 70 kD, while the most prominent came around 65 kD. Similarly single transfection with ATF5 alone was able to generate a single band on anti-His treatment (Fig 6.6B). Lysates from untransfected cells when treated with anti His antibody were not able to generate any such bands (blue boxes in Fig 6.6 A and B).

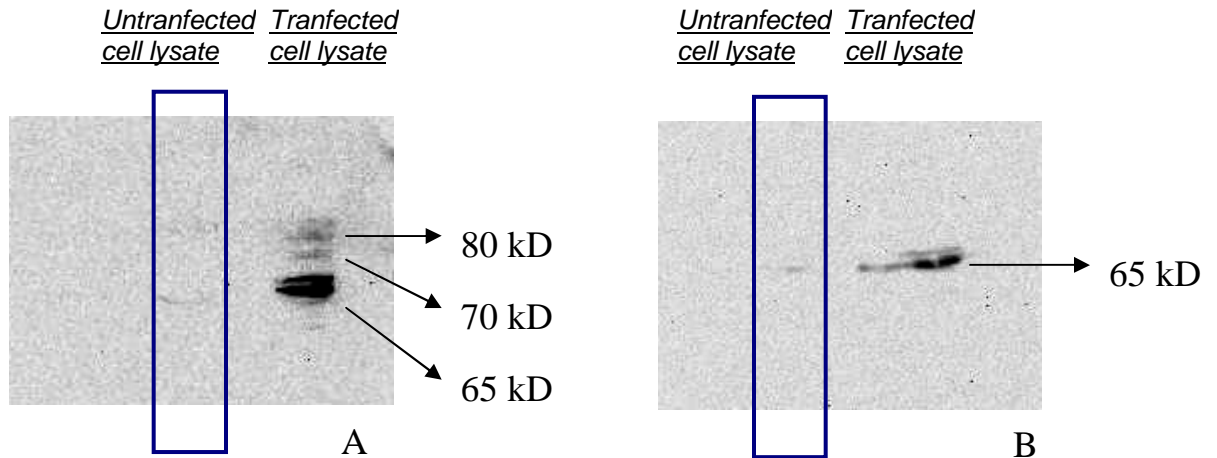


**Fig 6.6 – Anti-His immunoblotting of the HEK lysates.** The lysates obtained from cotransfected cells (Fig 6.6A) show three distinct bands at molecular weight 80, 70 and 65 kD. Cell lysates from single transfection with ATF5 (Fig 6.6B) show a single band at 65 kD. This can be compared to the lysates from untransfected control HEK cells (the areas shaded in the dark blue box) where no such bands could be seen.

### 6.3.5 Immunoblotting of the lysates with anti-ATF5 and anti-ATF4 antibodies

Immunoblotting of the cotransfected lysate with anti-ATF5 antibody was able to show a prominent band at 65 kD weight (Fig 6.7A), indicating that the band at 65 kD was indeed ATF5 protein. Similarly, immunoblotting with ATF4 was able to show two such distinct bands at 65 kD (Fig 6.7B)

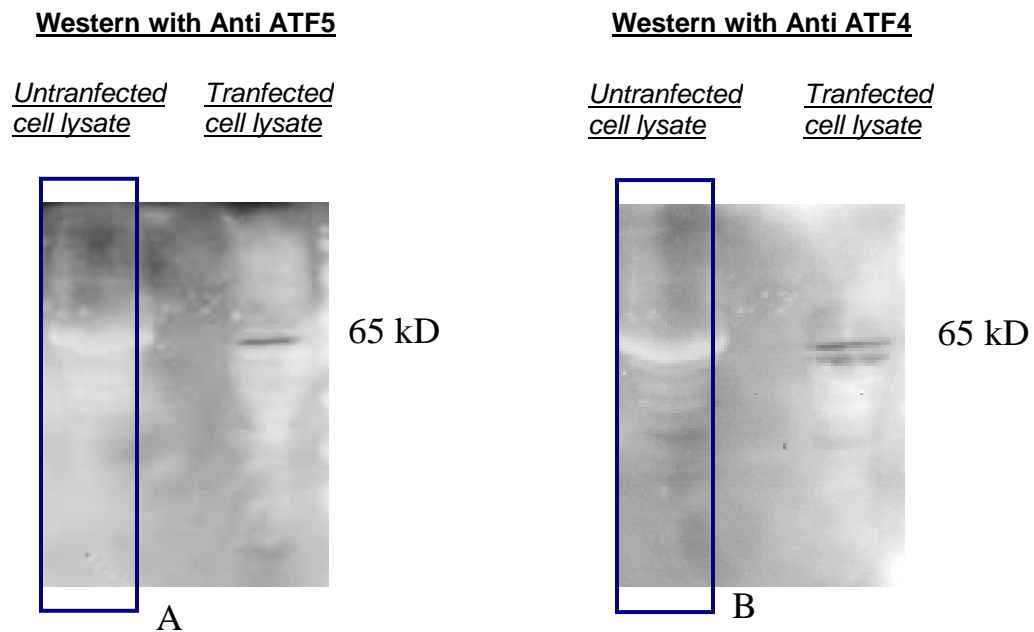


**Fig 6.7 – Anti-ATF5 and anti-ATF4 immunoblotting of the HEK lysates.** The lysates obtained from cotransfected cells show a single prominent band at 65 kD when immunoblotted with anti-ATF5 antibody (Fig 6.7 A). Immunoblotting of the same blot with anti-ATF4 showed two prominent bands at about the same weight (Fig 6.7 B). This is in comparison to untransfected controls which do not show any such bands (the area shaded with the dark blue box)

### 6.3.6 Immunoprecipitation with anti-ATF4; Western Blot with anti-ATF5

Immunoprecipitation with anti-ATF4 and subsequent immunoblotting with anti-ATF5 showed the presence of two distinct bands. The upper band lies at a molecular weight of around 65 kD, while the lower one lies at a molecular mark of 32 kD (Fig 6.8).

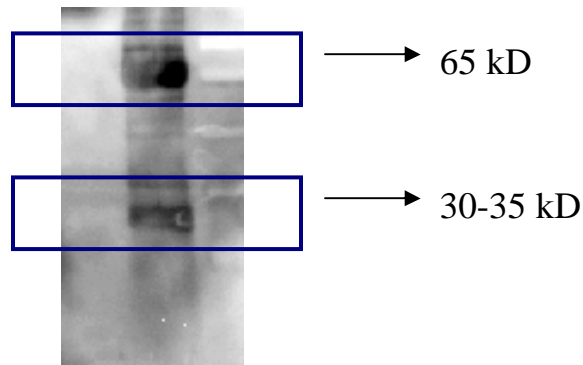


**Fig 6.8 – IP with anti-ATF4; WB with anti-ATF5.** The immunoblotting with anti-ATF5 showed the presence of two prominent bands. The heavier band was at molecular weight of 65 kD, while the lighter one was at around 32 kD.

### 6.3.7 Immunoprecipitation with anti-ATF5; Western Blot with anti-ATF4

Immunoprecipitation of the cell lysates with anti-ATF5 and subsequent immunoblotting with anti-ATF4 was able to show a distinct band of molecular weight 35 kD (Fig 6.9).

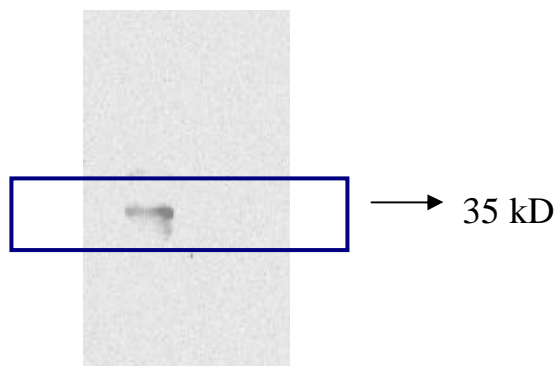


**Fig 6.9 – IP with anti-ATF5; WB with anti-ATF4.** The immunoblotting with anti-ATF4 showed the presence of a single, distinct band of molecular weight 35 kD.

## 6.4 DISCUSSION

Immunoprecipitation is one of the commonly used methods for demonstrating the ability of proteins to interact with one another. In this procedure the protein of interest is precipitated with Protein G beads initially using specific antibody. If there are any binding partners to this protein, they would also be pulled down by the first antibody and could be detected by a second antibody, specific to the binding partner.

To look for any interaction between ATF4 and ATF5, we decided to clone the two genes in a mammalian expression vector. The inserts that were generated by PCR from the Human MGC (Mammalian Gene Collection) cDNA clones for the respective proteins were of the correct base pair length (Fig 6.3 A, B and C). The subsequent transformation in Novablue™ cells was successful and we were able to isolate colonies that had taken up the right set of inserts (Fig 6.5). The plasmids isolated from these colonies were then cotransfected into HEK 293 cells. These cells have been used extensively for in vivo transfection and protein expression and have been known to yield consistently good transfection and expression efficiencies (Okamoto Y et al., 2005; Sauerwald TM et al., 2002).

Western blot done on the cell lysates with anti-His antibody showed three distinct bands (Fig 6.6 A). Anti-his antibody is very specific for detecting expressed proteins, as it binds to the unique repeats of histidine sequences seen in the expression tag, and thus cannot bind to the native histidine residues. The molecular weights detected were around 80 kD, 70 kD and 65 kD. The subsequent blotting with anti-ATF5 antibody was able to generate a band at the 65 kD mark. This implies that ATF5 proteins might be present at the 65 kD



mark. This is roughly twice the estimated molecular weight of ATF5, which is around 32 kD. A possible explanation for this finding maybe because the ATF5 in the cell lysates are being strongly bound to each other, generating a combination of homodimers. Also it may be possible that the other two bands seen at 75 kD and 80 kD maybe the outcome of such binding in the lysates. With the molecular weight of monomeric ATF4 being 39 kD, a homodimeric form could possibly have a molecular weight of around 78 kD (which could theoretically correspond to the highest band in Fig 6.6A. Similarly a heterodimer of ATF4 and ATF5 would be expected to have a molecular weight of 71 kD (39 + 32). The band seen at 75 kD could as well imply a heterodimer of ATF4 and ATF5. Though it could be presumed from this that ATF5 is forming dimers in the cell lysate, it would be rather premature to assert that the same occurs in vivo in the body. This is because small alterations in pH and ionic concentrations of the cell lysates may be enough to alter the affinity and binding properties of proteins. Another reason is that in vivo, these proteins are being expressed in very minute quantities. Situations like this, where proteins are being generated in large quantities, itself maybe enough to influence their binding properties.

When immunoprecipitation was done with anti-ATF4 and the pull down immunoblotted with anti-ATF5, two distinct bands were generated (Fig 6.8). The heavier band (at a molecular weight of 65 kD), corresponded to the one that was observed in Fig 6.6A. Along with this, a smaller band between 30 to 35 kD could also be seen. The heavier band could be the dimerized form of ATF5, just like the ones seen in the plain cell lysates. The smaller band, which was also detected with anti-ATF5 antibody, corresponds

to the molecular weight of ATF5 monomer predicted from our calculations (ie around 32 kD). It could be implied from these findings that immunoprecipitation with anti-ATF4 antibody was able to pull down with it two distinct bands of ATF5 proteins. The heavier band might be the homodimeric form of ATF5, while the lighter band could be the monomeric form of ATF5.

In the next phase, where immunoprecipitation was done with anti-ATF5 and western was done with anti-ATF4, we were able to pull down a protein having a molecular weight of around 35 kD (Fig 6.9). The presence of a single, distinct band being detected with anti-ATF4 would imply that the protein being detected here is the monomeric form of ATF4 itself. However, the molecular weight that is being seen here is lesser than that predicted for ATF4 (i.e. about 39 kD). This discrepancy may stem from the possibility that ATF4 protein may have undergone degradation or might have been prematurely cleaved, yielding a smaller fragment. At this point, it could be presumed that when ATF5 protein is being pulled down from cell lysates, ATF4 would be also be pulled out.

## **6.8 CONCLUSION**

When immunoprecipitation was done on these cell lysate containing expressed ATF4 and ATF5, ATF5 pull down resulted in co-precipitation of ATF4 and vice versa also, implying that these two proteins might have the possibility of interacting with each. If such a possibility exists, it might mean that this interaction could influence the manner in which ADSCs undergo osteogenic differentiation. However, this experiment is fraught with a few drawbacks, namely the inability to correctly mimic an in vivo environment.

Since this work was done on cell lysates having an abundance of the interacting proteins (unlike the physiological situation where these transcription factors are found in very low concentrations within the nucleus), it would be premature to arrive at the conclusion of the nature of interaction and hence the subsequent effects of these protein interactions. Even then, looking at the data from the gene silencing experiments and the cotransfection experiments, it could be gathered that ATF5 might have relevance in the osteogenic differentiation of ADSCs.

## **CHAPTER 7**

### **CONCLUSION AND FUTURE LINE OF WORK**

Human adipose tissue is a rich source of stromal cells. This work has shown that adipose tissue isolated from lipoaspirates of human donors can be processed to yield a population of stromal cells, called ADSCs, having unique properties. These cells when grown in cultures exposed to osteogenic stimuli showed markers suggesting commitment towards the osteogenic lineage. Alizarin red staining and Immunohistochemistry showed significantly visible differences between the osteo-induced and uninduced samples. These findings were corroborated by real time PCR which showed an increased expression of specific markers like osteocalcin and Runx2 in the osteo-induced groups. However, there was considerable variation in the gene expression pattern of osteopontin and osteonectin among different donor groups. The expression of the protein form of the above two genes gave a variable result in the western blot experiments. As explained in Chapter 4, such an inter donor variability in marker expression could be the outcome of several factors like , differential sampling techniques or functional differences in the osteogenic potential of the MSCs or variations in the physiological status of the patients.

Previous work done by Leong TWD had shown that one particular gene, known as ATF5, was consistently down regulated during osteogenic induction of ADSCs. As a continuation of this, the change in gene expression profile of ADSCs to osteogenic stimuli when the expression of ATF5 was silenced by RNA interference was observed. It

was observed that when ATF5 gene expression is silenced with siRNA, an increased expression of osteocalcin was seen in some of the ADSC, even in the absence of any inducing factors. The expression of another protein which has been implicated in mediating the process of osteogenesis in non-osteoblast cells, known as ATF4 was also studied. An increased expression of ATF4 was also seen in some, but not all the samples studied, which might be due to the intrinsic differences between the osteogenic capabilities of the different cell samples.

The subsequent cotransfection and immunoprecipitation experiments with ATF4 and ATF5 proteins showed that these two proteins have the potential to bind to each other. However, the shortcomings of these experiments were that they were done with cell lysates having proteins expressed in large quantities. The presence of an excess of proteins and the different buffering environment could have influenced the extent of interaction between the two proteins. Though the binding observed in the in vitro expressed proteins was not conclusive enough to prove that such a phenomenon does occur in vivo, this further strengthened the hypothesis that binding of ATF4 and ATF5 may indeed occur and influence the behavior of ADSCs under osteogenic conditions.

A better way of estimating the nature of interactions between transcription factors in vivo maybe to look at the nuclear extracts of native cells. However, the lower concentration of these factors in the nucleus might also influence the outcome of the experiments. A knock out model, in which there is targeted disruption of the genome, would bring about the phenotype change that occurs from the absence of protein expression. Profiling the

expression pattern of such a model would reveal those pathways and signals that come directly under the influence of the disrupted protein. Similarly, lentivirus mediated stable gene suppression would also bring about such an outcome, thus making it possible to focus in the right direction.

The findings in this thesis indicate that osteogenic induction of ADSCs is a property that varies among donor samples. Apart from the ATF family of proteins, there could be a number of other transcription factors that interplay to bring about osteogenesis in ADSCs. A clearer understanding of the molecular mechanisms would better identify critical pathways that could be modulated to this effect.

## BIBLIOGRAPHY

Amarzguioui M, Holen T, Babaie E, Prydz H. Tolerance for mutations and chemical modifications in a siRNA. *Nucleic Acids Res.* 2003; 15;31(2):589-95.

Ameri K, Harris AL. Activating transcription factor 4. *Int J Biochem Cell Biol.* 2007

Angelastro JM, Mason JL, Ignatova TN, Kukekov VG, Stengren GB, Goldman JE, Greene LA. Downregulation of activating transcription factor 5 is required for differentiation of neural progenitor cells into astrocytes. *J Neurosci.* 2005; 13;25(15):3889-99

Ashjian PH, Elbarbary AS, Edmonds B, DeUgarte D, Zhu M, Zuk PA, Lorenz HP, Benhaim P, Hedrick MH. In vitro differentiation of human processed lipoaspirate cells into early neural progenitors. *Plast Reconstr Surg.* 2003; 111(6):1922-31

Aust L, Devlin B, Foster SJ, Halvorsen YD, Hicok K, du LT, Sen A, Willingmyre GD, Gimble JM: Yield of human adiposederived adult stem cells from liposuction aspirates. *Cytotherapy* 2004; 6: 7–14

Barry FP, Murphy JM. Mesenchymal stem cells: clinical applications and biological characterization. *Int J Biochem Cell Biol.* 2004; 36(4):568-84.

Bernardo ME, Emons JA, Karperien M, Nauta AJ, Willemze R, Roelofs H, Romeo S, Marchini A, Rappold GA, Vukicevic S, Locatelli F, Fibbe WE. Human mesenchymal stem cells derived from bone marrow display a better chondrogenic differentiation compared with other sources. *Connect Tissue Res.* 2007; 48(3):132-40.

Black BL, Olson EN. Transcriptional control of muscle development by myocyte enhancer factor-2 (MEF2) proteins. *Annu Rev Cell Dev Biol.* 1998; 14:167-96.

Bruder SP, Horowitz MC, Mosca JD, Haynesworth SE. Monoclonal antibodies reactive with human osteogenic cell surface antigens. *Bone.* 1997; 21(3):225-35.

Bruder SP, Ricalton NS, Boynton RE, Connolly TJ, Jaiswal N, Zaia J, Barry FP. Mesenchymal stem cell surface antigen SB-10 corresponds to activated leukocyte cell adhesion molecule and is involved in osteogenic differentiation. *J Bone Miner Res.* 1998; 13(4):655-63.

Caplan AI. The mesengenic process. *Clin Plast Surg.* 1994; 21(3):429-35.

Chen D, Zhao M, Mundy GR. Bone morphogenetic proteins. *Growth Factors.* 2004; 22(4):233-41.

Chi JT, Chang HY, Wang NN, Chang DS, Dunphy N, Brown PO. Genomewide view of gene silencing by small interfering RNAs. *Proc Natl Acad Sci U S A.* 2003 ;100(11):6343-6.

Choi KY, Kim HJ, Lee MH, Kwon TG, Nah HD, Furuichi T, Komori T, Nam SH, Kim YJ, Kim HJ, Ryoo HM. Runx2 regulates FGF2-induced Bmp2 expression during cranial bone development. *Dev Dyn.* 2005; 233(1):115-21

Christakos S, Dhawan P, Liu Y, Peng X, Porta A. New insights into the mechanisms of vitamin D action. *J Cell Biochem.* 2003 ;88(4):695-705.

Cowan CM, Shi YY, Aalami OO, Chou YF, Mari C, Thomas R, Quarto N, Contag CH, Wu B, Longaker MT. Adipose-derived adult stromal cells heal critical-size mouse calvarial defects. *Nat Biotechnol.* 2004 ;22(5):560-7.

De Ugarte DA, Alfonso Z, Zuk PA, Elbarbary A, Zhu M, Ashjian P, Benhaim P, Hedrick MH, Fraser JK. Differential expression of stem cell mobilization-associated molecules on multi-lineage cells from adipose tissue and bone marrow. *Immunol Lett.* 2003; 89(2-3):267-70.

Di Rocco G, Iachininoto MG, Tritarelli A, Straino S, Zacheo A, Germani A, Crea F, Capogrossi MC. Myogenic potential of adipose-tissue-derived cells. *J Cell Sci.* 2006 ;119(Pt 14):2945-52

Dragoo JL, Choi JY, Lieberman JR, Huang J, Zuk PA, Zhang J, Hedrick MH, Benhaim P. Bone induction by BMP-2 transduced stem cells derived from human fat. *J Orthop Res.* 2003; 21(4):622-9.



Drissi H, Pouliot A, Stein JL, van Wijnen AJ, Stein GS, Lian JB. Identification of novel protein/DNA interactions within the promoter of the bone-related transcription factor Runx2/Cbfa1. *J Cell Biochem.* 2002; 86(2):403-12.

Ducy P, Zhang R, Geoffroy V, Ridall AL, Karsenty G. Osf2/Cbfa1: a transcriptional activator of osteoblast differentiation. *Cell.* 1997 ;89(5):747-54.

Ducy P. Cbfa1: a molecular switch in osteoblast biology. *Dev Dyn.* 2000 ;219(4):461-71.

Festy F, Hoareau L, Bes-Houtmann S, Pequin AM, Gonthier MP, Munstun A, Hoarau JJ, Cesari M, Roche R. Surface protein expression between human adipose tissue-derived stromal cells and mature adipocytes. *Histochem Cell Biol.* 2005; 124(2):113-21.

Fire A, Xu S, Montgomery MK, Kostas SA, Driver SE, Mello CC. Potent and specific genetic interference by double-stranded RNA in *Caenorhabditis elegans*. *Nature.* 1998 ;391(6669):806-11.

Fischer C, Johnson J, Stillwell B, Conner J, Cerovac Z, Wilson-Rawls J, Rawls A. Activating transcription factor 4 is required for the differentiation of the lamina propria layer of the vas deferens. *Biol Reprod.* 2004 ;70(2):371-8.

Frank O, Heim M, Jakob M, Barbero A, Schäfer D, Bendik I, Dick W, Heberer M, Martin I. Real-time quantitative RT-PCR analysis of human bone marrow stromal cells during osteogenic differentiation in vitro. *J Cell Biochem.* 2002;85(4):737-46

Gergen JP, Wieschaus EF. The localized requirements for a gene affecting segmentation in *Drosophila*: analysis of larvae mosaic for runt. *Dev Biol.* 1985;109(2):321-35.

Gornostaeva SN, Rzhaininova AA, Gol'dstein DV. Myogenesis in hemopoietic tissue mesenchymal stem cell culture. *Bull Exp Biol Med.* 2006;141(4):493-9.

Gronthos S, Franklin DM, Leddy HA, Robey PG, Storms RW, Gimble JM. Surface protein characterization of human adipose tissue-derived stromal cells. *J Cell Physiol.* 2001; 189(1):54-63.

Grove JE, Bruscia E, Krause DS. Plasticity of bone marrow-derived stem cells. *Stem Cells*. 2004; 22(4):487-500.

Hai T, Curran T. Cross-family dimerization of transcription factors Fos/Jun and ATF/CREB alters DNA binding specificity. *Proc Natl Acad Sci U S A*. 1999; 88(9):3720-4.

Hai T, Hartman MG. The molecular biology and nomenclature of the activating transcription factor/cAMP responsive element binding family of transcription factors: activating transcription factor proteins and homeostasis. *Gene*. 2001; 273(1):1-11.

Halvorsen YD, Franklin D, Bond AL, Hitt DC, Auchter C, Boskey AL, Paschalis EP, Wilkison WO, Gimble JM. Extracellular matrix mineralization and osteoblast gene expression by human adipose tissue-derived stromal cells. *Tissue Eng*. 2001 Dec; 7(6):729-41.

Hanai J, Chen LF, Kanno T, Ohtani-Fujita N, Kim WY, Guo WH, Imamura T, Ishidou Y, Fukuchi M, Shi MJ, Stavnezer J, Kawabata M, Miyazono K, Ito Y. Interaction and functional cooperation of PEBP2/CBF with Smads. Synergistic induction of the immunoglobulin germline  $\text{C}\alpha$  promoter. *J Biol Chem*. 1999; 274(44):31577-82.

Haynesworth SE, Baber MA, Caplan AI. Cytokine expression by human marrow-derived mesenchymal progenitor cells in vitro: effects of dexamethasone and IL-1  $\alpha$ . *J Cell Physiol*. 1996; 166(3):585-92.

Heinegård D, Oldberg A. Structure and biology of cartilage and bone matrix noncollagenous macromolecules. *FASEB J*. 1989; 3(9):2042-51

Hogan BL. Bone morphogenetic proteins: multifunctional regulators of vertebrate development. *Genes Dev*. 1996 (a); 10(13):1580-94

Hogan BL. Bone morphogenetic proteins in development. *Curr Opin Genet Dev*. 1996 (b); 6(4):432-8.

Jaiswal N, Haynesworth SE, Caplan AI, Bruder SP. Osteogenic differentiation of purified, culture-expanded human mesenchymal stem cells in vitro. *J Cell Biochem*. 1997; 64(2):295-312.

Karsenty G, Wagner EF. Reaching a genetic and molecular understanding of skeletal development. *Dev Cell*. 2002; 2(4):389-406.

Katz AJ, Tholpady A, Tholpady SS, Shang H, Ogle RC. Cell surface and transcriptional characterization of human adipose-derived adherent stromal (hADAS) cells. *Stem Cells*. 2005; 23(3):412-23.

Kimelman N, Pelled G, Helm GA, Huard J, Schwarz EM, Gazit D. Gene- and Stem Cell-Based Therapeutics for Bone Regeneration and Repair. *Tissue Eng*. 2007 x

Klees RF, Salaszyk RM, Kingsley K, Williams WA, Boskey A, Plopper GE. Laminin-5 induces osteogenic gene expression in human mesenchymal stem cells through an ERK-dependent pathway. *Mol Biol Cell*. 2005;16(2):881-90

Kobayashi T, Kronenberg H. Minireview: transcriptional regulation in development of bone. *Endocrinology*. 2005; 146(3):1012-7.

Komori T, Yagi H, Nomura S, Yamaguchi A, Sasaki K, Deguchi K, Shimizu Y, Bronson RT, Gao YH, Inada M, Sato M, Okamoto R, Kitamura Y, Yoshiki S, Kishimoto T. Targeted disruption of *Cbfa1* results in a complete lack of bone formation owing to maturational arrest of osteoblasts. *Cell*. 1997; 89(5):755-64.

Kondo M, Wagers AJ, Manz MG, Prohaska SS, Scherer DC, Beilhack GF, Shizuru JA, Weissman IL. Biology of hematopoietic stem cells and progenitors: implications for clinical application. *Annu Rev Immunol*. 2003; 21:759-806.

Krabbe C, Zimmer J, Meyer M. Neural transdifferentiation of mesenchymal stem cells--a critical review. *APMIS*. 2005;113(11-12):831-44.

Kurreck J. Antisense and RNA interference approaches to target validation in pain research. *Curr Opin Drug Discov Devel*. 2004; 7(2):179-87.

Lee JH, Rhie JW, Oh DY, Ahn ST. Osteogenic differentiation of human adipose tissue-derived stromal cells (hASCs) in a porous three-dimensional scaffold. *Biochem Biophys Res Commun*. 2008

Lee MH, Kim YJ, Kim HJ, Park HD, Kang AR, Kyung HM, Sung JH, Wozney JM, Kim HJ, Ryoo HM. BMP-2-induced Runx2 expression is mediated by Dlx5, and TGF-beta 1 opposes the BMP-2-induced osteoblast differentiation by suppression of Dlx5 expression. *J Biol Chem.* 2003; 278(36):34387-94.

Leong DT, Khor WM, Chew FT, Lim TC, Hutmacher DW. Characterization of osteogenically induced adipose tissue-derived precursor cells in 2-dimensional and 3-dimensional environments. *Cells Tissues Organs.* 2006;182(1):1-11.

Leong TWD, Characterization of human Adipose derived adult multipotent precursor cells – PhD Thesis, National University of Singapore, 2006

Li TS, Ito H, Hayashi M, Furutani A, Matsuzaki M, Hamano K. Cellular expression of integrin-beta 1 is of critical importance for inducing therapeutic angiogenesis by cell implantation. *Cardiovasc Res.* 2005; 65(1):64-72.

Luzi E, Marini F, Sala SC, Tognarini I, Galli G, Brandi ML. Osteogenic differentiation of human adipose tissue-derived stem cells is modulated by the miR-26a targeting of the SMAD1 transcription factor. *J Bone Miner Res.* 2008;23(2):287-95

Majumdar MK, Keane-Moore M, Buyaner D, Hardy WB, Moorman MA, McIntosh KR, Mosca JD. Characterization and functionality of cell surface molecules on human mesenchymal stem cells. *J Biomed Sci.* 2003; 10(2):228-41.

Masuoka HC, Townes TM. Targeted disruption of the activating transcription factor 4 gene results in severe fetal anemia in mice. *Blood.* 2002; 99(3):736-45.

Minguell JJ, Erices A, Conget P. Mesenchymal stem cells. *Exp Biol Med* 2001; 226(6):507-20.

Mizuno H, Zuk PA, Zhu M, Lorenz HP, Benhaim P, Hedrick MH. Myogenic differentiation by human processed lipoaspirate cells. *Plast Reconstr Surg.* 2002; 109(1):199-209; discussion 210-1.

Muschler GF, Nitto H, Boehm CA, Easley KA: Age- and gender-related changes in the cellularity of human bone marrow and the prevalence of osteoblastic progenitors. *J Orthop Res* 2001; 19: 117–125

Nakashima K, Zhou X, Kunkel G, Zhang Z, Deng JM, Behringer RR, de Crombrughe B. The novel zinc finger-containing transcription factor osterix is required for osteoblast differentiation and bone formation. *Cell*. 2002; 108(1):17-29.

Ogawa R, Mizuno H, Hyakusoku H, Watanabe A, Migita M, Shimada T, Chondrogenic and osteogenic differentiation of adipose-derived stem cells isolated from GFP transgenic mice, *J. Nippon. Med. Sch.* 71 (2004) 240– 241.

Okamoto Y, Morishita J, Wang J, Schmid PC, Krebsbach RJ, Schmid HH, Ueda N. Mammalian cells stably overexpressing N-acylphosphatidylethanolamine-hydrolysing phospholipase D exhibit significantly decreased levels of N-acylphosphatidylethanolamines. *Biochem J*. 2005; 389(Pt 1):241-7.

Ong SY, Dai H, Leong KW. Hepatic differentiation potential of commercially available human mesenchymal stem cells. *Tissue Eng*. 2006; 12(12):3477-85

Owen TA, Aronow M, Shalhoub V, Barone LM, Wilming L, Tassinari MS, Kennedy MB, Pockwinse S, Lian JB, Stein GS. Progressive development of the rat osteoblast phenotype in vitro: reciprocal relationships in expression of genes associated with osteoblast proliferation and differentiation during formation of the bone extracellular matrix. *J Cell Physiol*. 1990;143(3):420-30.

Philipsen S, Suske G. A tale of three fingers: the family of mammalian Sp/XKLF transcription factors. *Nucleic Acids Res*. 1999; 27(15):2991-3000.

Pittenger MF, Mackay AM, Beck SC, Jaiswal RK, Douglas R, Mosca JD, Moorman MA, Simonetti DW, Craig S, Marshak DR. Multilineage potential of adult human mesenchymal stem cells. *Science*. 1999 Apr 2; 284(5411):143-7.

Pomerantz J, Blau HM. Nuclear reprogramming: a key to stem cell function in regenerative medicine. *Nat Cell Biol*. 2004; 6(9):810-6.

Price PA, Baukol SA. 1,25-Dihydroxyvitamin D<sub>3</sub> increases synthesis of the vitamin K-dependent bone protein by osteosarcoma cells. *J Biol Chem*. 1980; 255(24):11660-3

Prufer K, Barsony J. Retinoid X receptor dominates the nuclear import and export of the unliganded vitamin D receptor. *Mol Endocrinol*. 2002; 16(8):1738-51.

Rodan GA, Noda M. Gene expression in osteoblastic cells. *Crit Rev Eukaryot Gene Expr.* 1991;1(2):85-98.

Salasznyk RM, Williams WA, Boskey A, Batorsky A, Plopper GE. Adhesion to Vitronectin and Collagen I Promotes Osteogenic Differentiation of Human Mesenchymal Stem Cells. *J Biomed Biotechnol.* 2004; (1):24-34.

Sauerwald TM, Betenbaugh MJ, Oyler GA. Inhibiting apoptosis in mammalian cell culture using the caspase inhibitor XIAP and deletion mutants. *Biotechnol Bioeng.* 2002; 77(6):704-16.

Scherer L, Rossi JJ. Therapeutic applications of RNA interference: recent advances in siRNA design. *Adv Genet.* 2004; 52:1-21.

Shore EM, Ahn J, Jan de Beur S, Li M, Xu M, Gardner RJ, Zasloff MA, Whyte MP, Levine MA, Kaplan FS. Paternally inherited inactivating mutations of the GNAS1 gene in progressive osseous heteroplasia. *N Engl J Med.* 2002; 346(2):99-106

Siddappa R, Licht R, van Blitterswijk C, de Boer J. Donor variation and loss of multipotency during in vitro expansion of human mesenchymal stem cells for bone tissue engineering. *J Orthop Res.* 2007;25(8):1029-41.

Skillington J, Choy L, Derynck R. Bone morphogenetic protein and retinoic acid signaling cooperate to induce osteoblast differentiation of preadipocytes. *J Cell Biol.* 2002; 159(1):135-46.

Strem BM, Hicok KC, Zhu M, Wulur I, Alfonso Z, Schreiber RE, Fraser JK, Hedrick MH. Multipotential differentiation of adipose tissue-derived stem cells. *Keio J Med.* 2005; 54(3):132-41.

Talens-Visconti R, Bonora A, Jover R, Mirabet V, Carbonell F, Castell JV, Gomez-Lechon MJ. Human mesenchymal stem cells from adipose tissue: Differentiation into hepatic lineage. *Toxicol In Vitro.* 2007; 21(2):324-9.

Thomas DM, Johnson SA, Sims NA, Trivett MK, Slavin JL, Rubin BP, Waring P, McArthur GA, Walkley CR, Holloway AJ, Diyagama D, Grim JE, Clurman BE, Bowtell DD, Lee JS, Gutierrez GM, Piscopo DM, Carty SA, Hinds PW. Terminal osteoblast differentiation, mediated by runx2 and p27KIP1, is disrupted in osteosarcoma. *J Cell Biol.* 2004; 167(5):925-34.

Timper K, Seboek D, Eberhardt M, Linscheid P, Christ-Crain M, Keller U, Muller B, Zulewski H. Human adipose tissue-derived mesenchymal stem cells differentiate into insulin, somatostatin, and glucagon expressing cells. *Biochem Biophys Res Commun.* 2006; 341(4):1135-40.

Tontonoz P, Graves RA, Budavari AI, Erdjument-Bromage H, Lui M, Hu E, Tempst P, Spiegelman BM. Adipocyte-specific transcription factor ARF6 is a heterodimeric complex of two nuclear hormone receptors, PPAR gamma and RXR alpha. *Nucleic Acids Res.* 1994; 22(25):5628-34.

Verfaillie C, Hurley R, Bhatia R, McCarthy JB. Role of bone marrow matrix in normal and abnormal hematopoiesis. *Crit Rev Oncol Hematol.* 1994; 16(3):201-24.

Villaron EM, Almeida J, Lopez-Holgado N, Alcoceba M, Sanchez-Abarca LI, Sanchez-Guijo FM, Alberca M, Perez-Simon JA, San Miguel JF, Del Canizo MC. Mesenchymal stem cells are present in peripheral blood and can engraft after allogeneic hematopoietic stem cell transplantation. *Haematologica.* 2004; 89(12):1421-7.

Verettas DA, Galanis B, Kazakos K, Hatzayiannakis A, Kotsios E. Fractures of the proximal part of the femur in patients under 50 years of age. *Injury.* 2002;33(1):41-5.

Vickers TA, Koo S, Bennett CF, Crooke ST, Dean NM, Baker BF. Efficient reduction of target RNAs by small interfering RNA and RNase H-dependent antisense agents. A comparative analysis. *J Biol Chem.* 2003; 278(9):7108-18.

Wu Z, Bucher NL, Farmer SR. Induction of peroxisome proliferator-activated receptor gamma during the conversion of 3T3 fibroblasts into adipocytes is mediated by C/EBPbeta, C/EBPdelta, and glucocorticoids. *Mol Cell Biol.* 1996; 16(8):4128-36.

Xiao G, Jiang D, Ge C, Zhao Z, Lai Y, Boules H, Phimphilai M, Yang X, Karsenty G, Franceschi RT. Cooperative interactions between activating transcription factor 4 and Runx2/Cbfa1 stimulate osteoblast-specific osteocalcin gene expression. *J Biol Chem.* 2005; 280(35):30689-96.

Yanez R, Lamana ML, Garcia-Castro J, Colmenero I, Ramirez M, Bueren JA. Adipose tissue-derived mesenchymal stem cells have in vivo immunosuppressive properties applicable for the control of the graft-versus-host disease. *Stem Cells.* 2006; 24(11):2582-91

Yang X, Matsuda K, Bialek P, Jacquot S, Masuoka HC, Schinke T, Li L, Brancorsini S, Sassone-Corsi P, Townes TM, Hanauer A, Karsenty G. ATF4 is a substrate of RSK2 and an essential regulator of osteoblast biology; implication for Coffin-Lowry Syndrome. *Cell.* 2004 (a) ; 117(3):387-98.

Yang X, Karsenty G. ATF4, the osteoblast accumulation of which is determined post-translationally, can induce osteoblast-specific gene expression in non-osteoblastic cells. *J Biol Chem.* 2004 (b) ; 279(45):47109-14. (b)

Yoon E, Dhar S, Chun DE, Gharibjanian NA, Evans GR. In vivo osteogenic potential of human adipose-derived stem cells/poly lactide-co-glycolic acid constructs for bone regeneration in a rat critical-sized calvarial defect model. *Tissue Eng.* 2007;13(3):619-27.

Zhang YW, Yasui N, Ito K, Huang G, Fujii M, Hanai J, Nogami H, Ochi T, Miyazono K, Ito Y. A RUNX2/PEBP2alpha A/CBFA1 mutation displaying impaired transactivation and Smad interaction in cleidocranial dysplasia. *Proc Natl Acad Sci U S A.* 2000; 97(19):10549-54

Zuk PA, Zhu M, Ashjian P, De Ugarte DA, Huang JI, Mizuno H, Alfonso ZC, Fraser JK, Benhaim P, Hedrick MH. Human adipose tissue is a source of multipotent stem cells. *Mol Biol Cell.* 2002; 13(12):4279-95.